Turkish Journal of Earth Sciences (Turkish J. Earth Sci.), **Vol. 13**, 2004, pp. 37-61. *Copyright ©TÜBİTAK*

Geochemistry and Geochronology of Orthogneisses in the Derbent (Alaşehir) Area, Eastern Part of the Ödemiş–Kiraz Submassif, Menderes Massif: Pan-African Magmatic Activity

O. ERSİN KORALAY[1], O. ÖZCAN DORA[1], FUKUN CHEN[2], MUHARREM SATIR[3] & OSMAN CANDAN[1]

[1] Dokuz Eylül University, Faculty of Engineering, Department of Geology, TR–35100 Bornova, İzmir - Turkey
(e-mail: ersin.koralay@deu.edu.tr)
[2] Insitute of Geology and Geophysics, Chinese Academy of Sciences
P.O. Box 9825, Beijing 100029 - China
[3] Eberhard-Karls-Universität Tübingen, Institut für Mineralogie, Petrologie und Geochemie
Lehrstuhl für Geochemie, Wilhelmstraße 56, 72074 Tübingen - Germany

Abstract: Pan-African basement rocks and the Palaeozoic cover series of the Menderes Massif are exposed around Derbent (Alaşehir) in the eastern part of the Ödemiş-Kiraz submassif. Garnet-mica schists of the Pan-African basement are intruded by the protoliths of orthogneisses and Triassic leucocratic orthogneisses. This study focuses on the geochronology and geochemistry of orthogneisses related to the Pan-African evolution of the Menderes Massif in latest Proterozoic time. Geochemical data suggest that the orthogneisses were derived from S-type, peraluminous, syn- to post-collisional granitoids of calc-alkaline affinity. Zircon grains from the orthogneisses, which are euhedral with typical igneous morphologies, were dated by the Pb-Pb evaporation method. Single zircon ages of two samples yielded $^{207}Pb/^{206}Pb$ ages of 561.5±1.8 Ma and 570.5±2.2 Ma. These ages are interpreted as the time of protolith emplacement of the orthogneisses. This major magmatic episode of the Menderes Massif can be attributed the Pan-African Orogeny which was related to the closure of the ocean basins and amalgamation of East and West Gondwana.

Key Words: orthogneiss, geochemistry, Pb–Pb zircon dating, Pan-African, Menderes Massif, Turkey

Menderes Masifi, Ödemiş–Kiraz Asmasifi Doğusunda Derbent (Alaşehir) Yöresinde Yer Alan Ortognaysların Jeokimyası ve Jeokronolojisi: Pan-Afrikan Magmatik Aktivite

Özet: Menderes Masifi'nin Pan-Afrikan yaşlı temel kayaları ve Paleozoyik örtü serileri Ödemiş-Kiraz asmasifi'nin doğusunda yer alan Derbent (Alaşehir) çevresinde yüzlek vermektedir. Pan-Afrikan temele ait granat-mika şistler, ortognayslar ve Triyas yaşlı lökokratik ortognaysların ilksel kayaları tarafından intrüze olmuşlardır. Bu çalışma, Proterozoyik sonunda Menderes Masifi'nin Pan-Afrikan evrimiyle ilişkili olan ortognaysların jeokimyası ve jeokronolojisi üzerinedir. Jeokimyasal veriler ortognaysların S-tipli, peralumino ve kalkalkalen karakterli, sin-/post-tektonik granitoyidlerden türediğini göstermektedir. Ortognayslardan ayrılan tipik magmatik ve öz şekilli zirkonlardan Pb-Pb evaporasyon yöntemiyle yaş tayinleri yapılmıştır. İki örneğin tek zirkon $^{207}Pb/^{206}Pb$ yaşları ortalama 561.5±1.8 my ve 570.5±2.2 my olarak elde edilmiştir. Bu yaşlar ortognaysların ilksel kayalarının sokulum yaşı olarak yorumlanmıştır. Menderes Masifi'ndeki bu ana magmatik olay okyanus havzalarının kapanması ve Doğu ve Batı Gondvana'nın çarpışmasına bağlantılı Pan-Afrikan orojeneziyle ilişkilendirilebilir.

Anahtar Sözcükler: ortognays, jeokimya, Pb–Pb zirkon yaş tayini, Pan-Afrikan, Menderes Masifi, Türkiye

Introduction

The Menderes Massif, which is elliptical and oriented NE–SW, has had significant impact on the geological evolution of western Anatolia. It is tectonically overlain by nappes of the İzmir-Ankara Zone (including the Bornova Flysch Zone of olistostromal character) in the northwest, the Afyon Zone (consisting of low-grade metapelite and metacarbonate rocks) in the north, and the Lycian Nappes

(comprising low-grade phyllites and carbonates and thick ophiolite slices in the south) (Figure 1) (Şengör & Yılmaz 1981; Okay 1986; Dora *et al.* 1995). The Menderes Massif has commonly been interpreted as the eastward continuation of the Attic-Cycladic Massif in the Aegean Sea (Dürr *et al.* 1978; Jacobshagen 1986; Oberhänsli *et al.* 1998). However, recently it has been suggested that the two massifs are not in all aspects related (Ring *et al.* 1999).

In early studies, it was considered that the Menderes Massif had a simple internal structure, made up of a Precambrian basement and an Early Palaeozoic to Early Tertiary cover series (Schuiling 1962). However, recent studies have shown that the Massif does not have a simple structure, and is characterised by nappe-stacking related to Alpine compressional tectonics in the Early Tertiary (Konak *et al.* 1994; Dora *et al.* 1994; Partzsch *et al.* 1998; Gessner *et al.* 2001a, 2001b; Ring *et al.* 1999). Compressional deformation fabrics have been overprinted by continental extension tectonics since the Oligocene–Miocene (Seyitoğlu *et al.* 1992, 2000, 2002; Bozkurt & Park 1994, 1997a, 1997b, 1999; Hetzel *et al.* 1995a, 1995b; Koçyiğit *et al.* 1999; Bozkurt & Satır 2000; Bozkurt 2000, 2001a, 2001b, 2002, 2003; Bozkurt & Oberhänsli 2001; Gessner *et al.* 2001c; Işık & Tekeli 2001; Lips *et al.* 2001; Ring *et al.* 2001, 2003; Sözbilir 2001, 2002; Özer & Sözbilir 2003; Işık *et al.* 2003; Ring & Lawyer 2003; Bozkurt & Sözbilir 2004). In spite of its complex tectonic structure, the Menderes Massif can be divided into two main rock associations

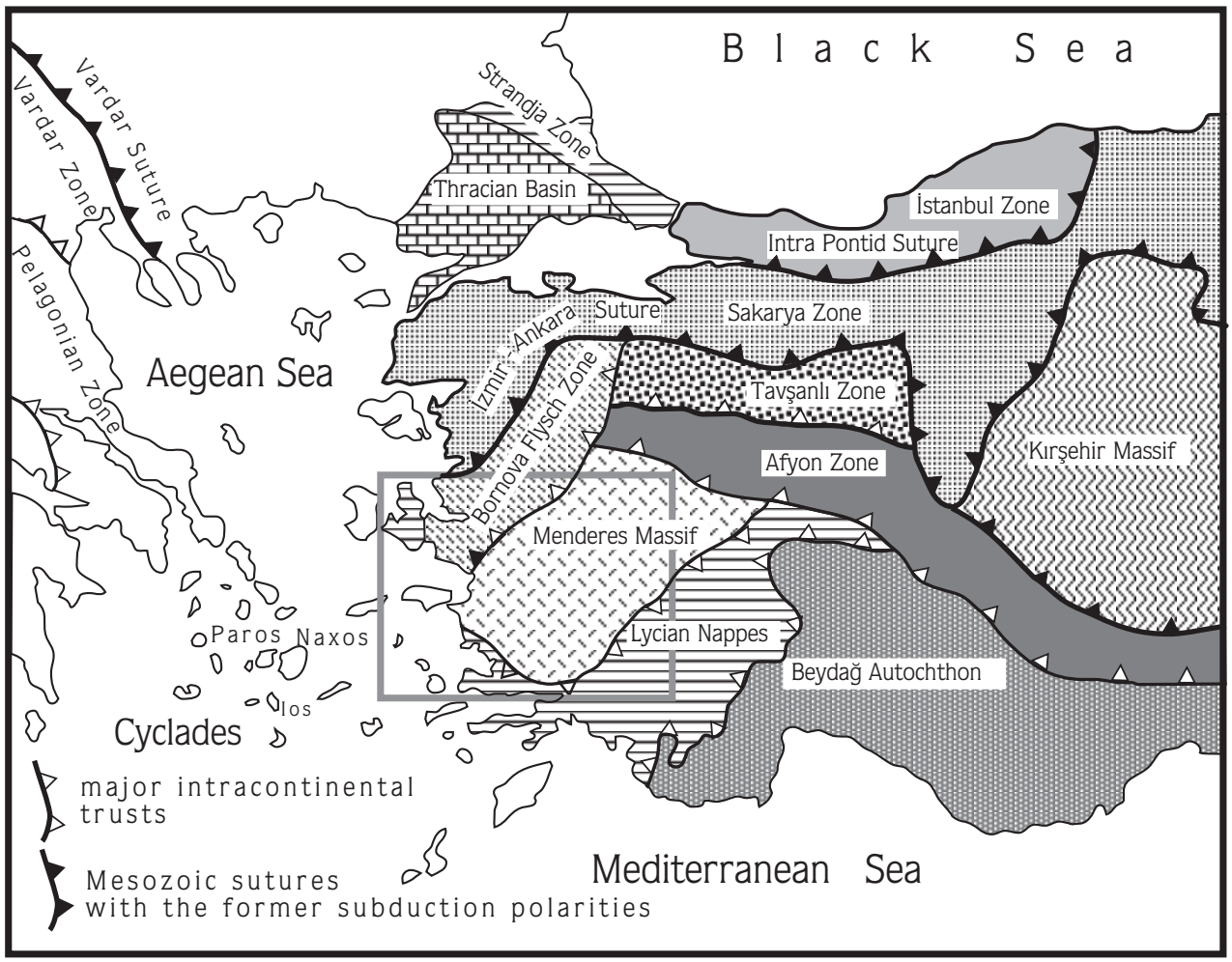

Figure1. Tectonic map of western Turkey and surrounding regions showing major continental blocks and tectonic zones (modified after Okay *et al.* 1996).

(Dora *et al.* 1995): (i) Pan-African basement rocks and (ii) Palaeozoic and Mesozoic–Early Tertiary cover series. The Pan-African basement is comprised partly of migmatised Late Proterozoic clastic metasediments (Koralay *et al.* 2003), i.e. paragneisses and mica schists, which are intruded by the protoliths of Precambrian eclogitic metagabbros and syn- to post-Pan-African orthogneisses. The basement rocks were subjected to polyphase metamorphism at granulite-, eclogite-, and amphibolite-facies conditions related to Pan-African orogenesis at the Precambrian-Cambrian boundary (Candan 1995, 1996; Dora *et al.* 1995; Oberhänsli *et al.* 1997; Candan & Dora 1998; Candan *et al.* 2000, 2001).

The cover series of the Menderes Massif can be subdivided into two units consisting of Palaeozoic and Mesozoic–Early Tertiary rocks. The Palaeozoic series is made up predominantly of a sequence of quartzite, phyllite and marble (Çağlayan *et al.* 1980; Konak *et al.* 1987; Bozkurt 1996; Okay 2001, 2002; Özer *et al.* 2001; Güngör & Erdoğan 2002; Whitney & Bozkurt 2002; Régnier *et al.* 2003; Rimmelé *et al.* 2003a, 2003b). The Mesozoic–Early Tertiary series comprises a sequence of metaconglomerate, schist, dolomite, and platform-type metacarbonate rocks with emery-metabauxite lenses, pelagic marble and metaolistostrome (Dürr 1975; Konak *et al.* 1987; Bozkurt 1994, 1996; Dora *et al.* 1995; Bozkurt & Park 1994, 1999; Ring *et al.* 1999, 2001, 2003; Okay 2001, 2002; Özer *et al.* 2001; Güngör & Erdoğan 2002; Whitney & Bozkurt 2002; Régnier *et al.* 2003; Rimmelé *et al.* 2003a, 2003b).

Geologic and geochronological evidence suggests that there have been three distinct phases of magmatic activity in the Menderes Massif: (i) Pan-African (Precambrian/Cambrian), (ii) Triassic and (iii) Tertiary. The major phase of magmatic activity, represented by the protoliths of the orthogneisses, took place at the Late Precambrian/Early Cambrian boundary (Hetzel & Reischmann 1996; Loos & Reischmann 1999; Dannat 1997; Hetzel *et al.* 1998; Gessner *et al.* 2001b, 2004). Granitic protoliths of the leucocratic orthogneisses, dated at about 235–246 Ma (Triassic), represent the second pulse of magmatic activity in the Menderes Massif (Dannat 1997; Koralay 2001; Koralay *et al.* 2001). The third phase of magmatic activity, represented by non-metamorphic granites and kersantites, has yielded ages of 25 to 12 Ma (United Nations 1974; Hetzel *et al.* 1995a).

Although a striking increase in the number of geochronological studies of the orthogneisses have been carried out during the last ten years (Hetzel & Reischmann 1996; Dannat 1997; Dannat & Reischmann 1998; Hetzel *et al.* 1998; Loos & Reischmann 1999; Gessner *et al.* 2001b, 2001c, 2004), only a limited number of detailed geochemical studies has been done on the orthogneisses, especially at the southern part of Çine submassif (Kun 1983; Kun & Candan 1987; Bozkurt 1994; Bozkurt *et al.* 1992, 1993, 1995; Dannat 1997).

In this study, the orthogneisses exposed around Derbent in the eastern part of the Ödemiş-Kiraz submassif were sampled and analysed in terms of geochemical and geochronological features. The aims of this paper are to: (a) present age determinations for intrusion of the orthogneisses obtained using the $^{207}Pb/^{206}Pb$ single-zircon evaporation method; (b) discuss the possible relationship of this magmatic event to the Pan-African metamorphic history of the Menderes Massif and; (c) show the geochemical characteristics of the orthogneiss and thereby discuss the possible source and tectonic environment of magma generation.

Geology

The study area is located in the eastern part of the Ödemiş-Kiraz submassif (Figure 2). In the vicinity of Derbent, the rock succession of the metamorphic series is made up of four nappe units (Figures 3 & 4). In ascending order, the first three nappe units formed by internal imbrications of the Pan-African basement series, whereas the uppermost nappe unit belongs to the Late Palaeozoic–Mesozoic cover series. The lowermost nappe unit of the Pan-African basement is made up entirely of garnet-mica schist. The middle nappe unit comprises predominantly garnet-mica schist that contains thin carbonate horizons. These schists are intruded by orthogneisses with well-preserved intrusive contact relationships (Figure 5). Furthermore, in the same nappe unit, the garnet-mica schist are also intruded by protoliths of Triassic leucocratic orthogneisses, dated at 235–246 Ma using the single zircon evaporation method (Koralay *et al.* 2001). The upper nappe slice of the Pan-African basement consists predominantly of orthogneisses. Only locally, the orthogneisses display intrusive contact relationships with partially migmatised paragneisses. The Pan-African nappe units are overlain by

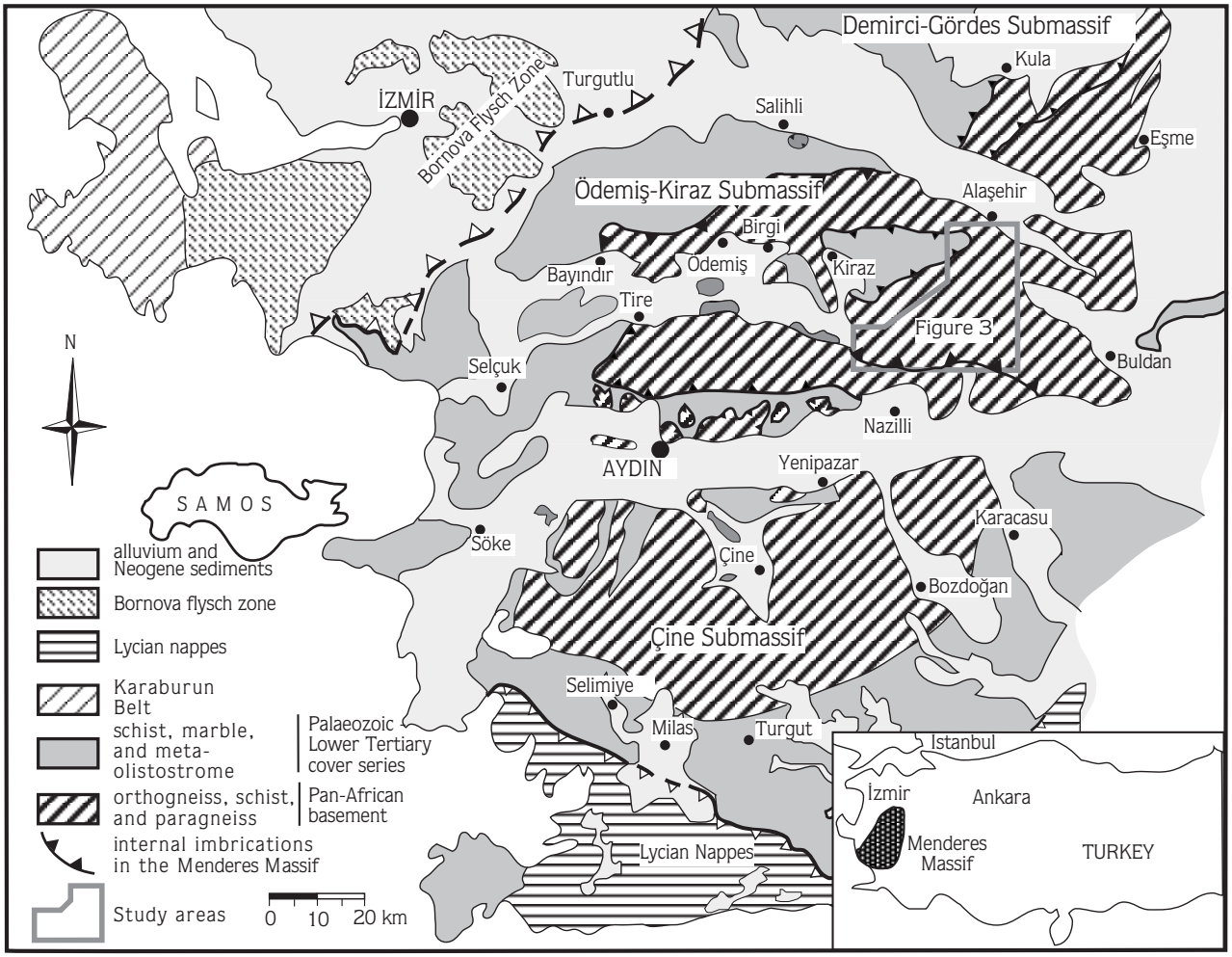

Figure 2. Simplified geological map of the Menderes Massif and location of the study area (modified after Candan 1995). See Figure 1 for location.

the cover series, the uppermost nappe unit, with a tectonic contact (Figure 3). The cover series can be divided into two units: (i) Palaeozoic (Permo–Carboniferous) unit which is made up of phyllite-quartzite-marble intercalation and (ii) Mesozoic (Cretaceous) sequence consisting of platform-type metacarbonate. The metamorphic rocks of the Menderes Massif are tectonically overlain by non-metamorphic and ophiolitic rocks of the İzmir-Ankara Zone. It is suggested that the structure of this nappe pile is related to crustal thickening in the Menderes Massif, which resulted from Alpine compressional tectonics (Dora *et al.* 1995; Partzsch *et al.* 1998).

Geochemistry

Fourteen representative samples of the orthogneisses (Figure 3) were analysed for 10 major- element oxides and 12 trace elements (Table 1). Major and trace elements were analysed from fused discs and on pressed powder pellets using Phillips PW 1130 X-ray fluorescence spectrometers calibrated against both international and in-house standards of appropriate compositions at the University of Tübingen, Germany.

Since the rocks have undergone amphibolite-facies metamorphism (Koralay *et al.* 1998; Candan *et al.* 2000) and experienced other secondary alteration processes, it is likely that most of the elements may have been

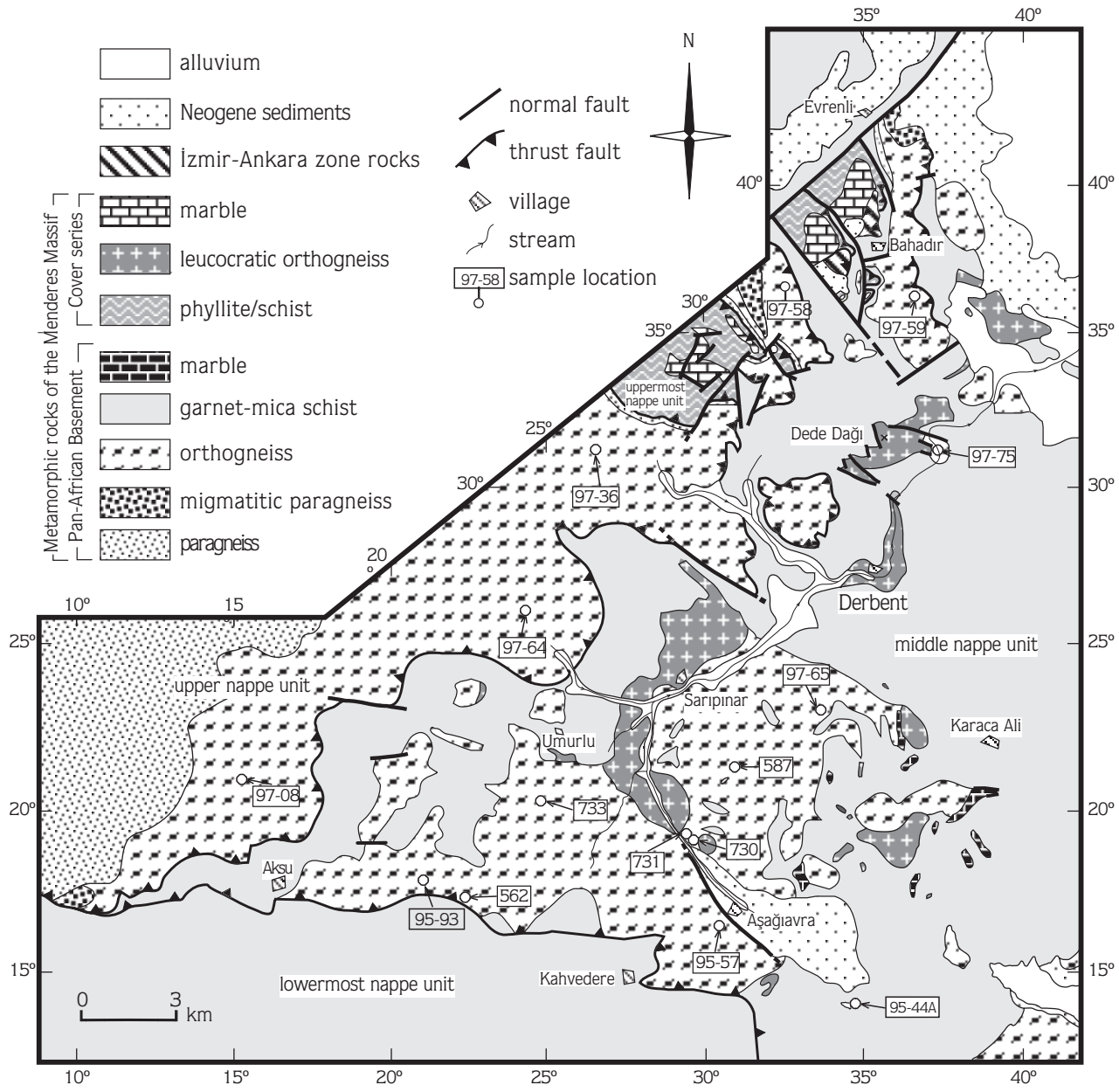

Figure 3. Geological map of the Derbent region, located in the eastern part of the Ödemiş-Kiraz submassif of the Menderes Massif. National grids: İzmir L20-b3, İzmir L20-c2, İzmir L20-c3, İzmir L20-c4, Uşak L21-a4, Uşak L21-d1, Uşak L21-d4.

mobilised. Major and selected trace elements were plotted against SiO_2 (wt%) values to establish their relative mobility (Figure 6). The orthogneisses are characterised by moderate to high silica contents (67–76 wt% SiO_2) and moderate alumina values (13–16 wt% Al_2O_3). Harker diagrams (Figure 6) show clear trends for most major and trace elements. On the SiO_2 variation diagrams, TiO_2, Al_2O_3, Fe_2O_3 and MgO show strong negative correlation. Na_2O shows a small data spread and negative correlation, whereas K_2O exhibits limited data scatter and positive correlation. Na and K are often highly mobile elements during metamorphism and weathering (e.g., Pearce 1976) but Na_2O–SiO_2 and K_2O–SiO_2 diagrams show limited data scatter and good correlation.

Table 1. Major- and trace-element analyses and normative data from orthogneiss samples, Ödemiş-Kiraz submassif, Menderes Massif. na– not analysed.

SAMPLE	562	587	730	731	733	95-44A	95-57	95-93	97-08	97-36	97-58	97-59	97-61	97-64	97-65	97-66	97-70	97-75
Major Oxides (wt %)																		
SiO_2	67.24	69.48	71.12	71.21	72.01	68.72	68.03	66.93	69.13	75.92	66.88	73.59	68.1	74.23	70.21	69.55	69.86	71.59
TiO_2	0.73	0.36	0.41	0.36	0.36	0.49	0.47	0.73	0.61	0.13	0.71	0.21	0.79	0.21	0.41	0.54	0.71	0.32
Al_2O_3	15.87	14.73	14.26	14.5	14.03	15.1	15.61	16.32	14.95	13.07	15.03	13.63	14.82	13.94	14.45	14.7	14.71	14.67
Fe_2O_3	4.67	3.65	3.11	2.77	2.52	3.59	3.54	4.11	3.96	1.03	4.97	1.33	4.33	1.21	2.93	3.64	3.22	2.28
MnO	0.02	0.06	0.05	0.05	0.05	0.08	0.04	0.07	0.05	0.02	0.06	0.02	0.04	0.01	0.04	0.06	0.03	0.02
MgO	1.53	0.65	0.53	0.49	0.47	0.63	0.72	1.02	1.35	0.28	1.82	0.33	2.18	0.30	0.62	0.99	1.63	0.44
CaO	0.66	1.43	1.31	1.28	0.27	0.43	1.27	1.81	1.86	0.61	1.51	0.76	1.81	0.52	1.53	0.67	1.86	0.63
Na_2O	4.29	3.56	3.54	3.60	3.50	3.93	3.55	3.72	2.83	2.72	2.72	2.52	4.03	2.30	3.10	2.33	3.58	2.23
K_2O	3.35	4.65	4.56	4.80	5.15	4.33	4.29	4.09	3.86	5.04	3.15	5.04	1.78	5.06	4.72	5.49	2.31	5.19
P_2O_5	na	na	na	na	na	na	0.14	na	0.16	0.17	0.24	0.08	0.17	0.07	0.23	0.29	0.16	0.18
LOI	1.54	0.99	0.88	0.83	1.02	1.66	1.31	0.92	0.98	0.68	2.33	0.99	1.41	1.54	0.95	1.21	1.37	2.15
Total	99.9	99.56	99.77	99.89	99.38	98.96	98.97	99.72	99.73	99.66	99.42	98.49	99.45	99.38	99.18	99.47	99.42	99.71
Trace Elements (ppm)																		
Ba	806	756	669	709	731	678	860	859	808	262	586	498	437	447	944	1036	407	679
Cr	45	42	33	24	23	37	-	34	39	4	63	30	28	-	4	22	34	-
Ga	16	16	16	15	16	17	-	17	na	na	na	na	na	na	na	na	na	na
Nb	19	20	21	18	17	20	16	18	13	4	12	3	14	6	12	25	15	17
Ni	na	na	na	na	na	na	-	-	10	-	26	5	13	-	3	12	5	1
Rb	70	54	133	126	134	117	141	98	131	142	110	138	82	158	134	194	128	170
Sr	108	146	139	140	87	109	143	148	162	106	161	98	144	99	154	164	240	101
Th	28	10	7	3	2	28	-	8	na	na	na	na	na	na	na	na	na	na
V	na	na	na	na	na	na	30	na	59	11	88	6	76	8	28	42	74	23
Y	27	17	43	43	34	33	56	47	22	46	37	36	48	35	44	42	23	22
Zn	na	na	na	na	na	na	64	na	61	23	93	24	25	23	62	120	26	61
Zr	285	284	239	234	246	212	316	255	212	70	220	123	258	117	272	260	270	171
Ratios																		
A/NK	2.08	1.79	1.76	1.73	1.62	1.83	1.99	2.09	2.24	1.68	2.56	1.80	2.55	1.89	1.85	1.88	2.50	1.98
A/CNK	1.91	1.53	1.52	1.50	1.57	1.74	1.71	1.70	1.75	1.56	2.04	1.64	1.95	1.77	1.55	1.73	1.90	1.82
F/F+Mg	0.75	0.85	0.85	0.85	0.84	0.85	0.83	0.80	0.75	0.79	0.73	0.80	0.67	0.80	0.83	0.79	0.66	0.84
F/Mg	3.05	5.62	5.87	5.65	5.36	5.70	4.95	4.03	2.94	3.67	2.74	4.05	1.99	4.03	4.76	3.67	1.97	5.18
Mg/F	6.20	4.30	3.64	3.26	2.99	4.22	4.26	5.13	5.31	1.31	6.79	1.66	6.51	1.51	3.55	4.64	4.84	2.72
Mg/Ca	2.32	0.45	0.40	0.38	1.74	1.47	0.56	0.56	0.72	0.46	1.20	0.43	1.20	0.57	0.40	1.48	0.88	0.69
Na/Ca	6.50	2.49	2.70	2.81	12.96	9.14	2.80	2.06	1.52	4.43	1.81	3.32	2.22	4.41	2.03	3.47	1.92	3.52
Na/K	1.28	0.77	0.78	0.75	0.68	0.91	0.83	0.91	0.73	0.54	0.86	0.50	2.27	0.45	0.66	0.42	1.55	0.43
Nb/Y	0.70	1.17	0.48	0.42	0.51	0.6	0.29	0.39	0.59	0.09	0.32	0.08	0.29	0.17	0.27	0.6	0.65	0.77
Rb/Sr	0.64	0.37	0.96	0.9	1.54	1.07	0.99	0.66	0.81	1.34	0.68	1.41	0.57	1.60	0.87	1.18	0.53	1.68
Rb/Zr	0.24	0.19	0.56	0.54	0.55	0.55	0.45	0.38	0.62	2.03	0.50	1.12	0.32	1.35	0.49	0.75	0.47	0.99
Rb/Ba	0.09	0.07	0.20	0.18	0.18	0.17	0.16	0.11	0.16	0.54	0.19	0.28	0.19	0.35	0.14	0.19	0.31	0.25
K/Rb	482.01	854.78	342.09	380.35	383.18	368.82	304.26	419.06	294.43	354.93	286.45	365.14	216.59	320.38	351.87	282.73	180.55	305.41
Zr/TiO_2	0.04	0.08	0.06	0.07	0.07	0.04	0.07	0.04	0.04	0.06	0.03	0.06	0.03	0.06	0.07	0.05	0.04	0.05
Selected Normative Components																		
Q	25.77	26.94	29.48	28.43	30.66	27.43	24.24	30.54	32.36	39.58	33.71	37.73	31.24	40.13	30.58	32.89	34.22	37.22
C	3.99	1.24	1.12	1.05	2.21	3.17	2.48	2.43	3.12	2.43	4.97	2.83	3.39	3.91	2.01	4.40	3.30	4.65
Or	19.80	27.48	26.95	28.37	30.43	25.59	24.17	29.78	22.79	29.78	18.62	29.78	10.50	29.91	27.86	32.41	13.66	30.68
Ab	36.30	30.12	29.95	30.46	29.62	33.25	31.48	22.97	23.95	22.97	23.04	21.33	34.06	19.45	26.25	19.72	30.28	18.9
An	3.27	7.09	6.50	6.35	1.34	2.13	8.98	1.94	8.20	1.94	5.93	3.28	7.88	2.11	6.08	1.45	8.22	1.98
An+Ab	39.57	37.21	36.00	36.81	30.96	35.38	40.46	24.91	32.15	24.91	28.97	24.61	41.94	21.56	32.33	21.17	38.5	20.88
An+Or	23.07	34.57	33.45	34.72	31.77	27.72	33.15	31.72	30.99	31.72	24.55	33.06	18.38	32.02	33.94	33.86	21.88	32.66

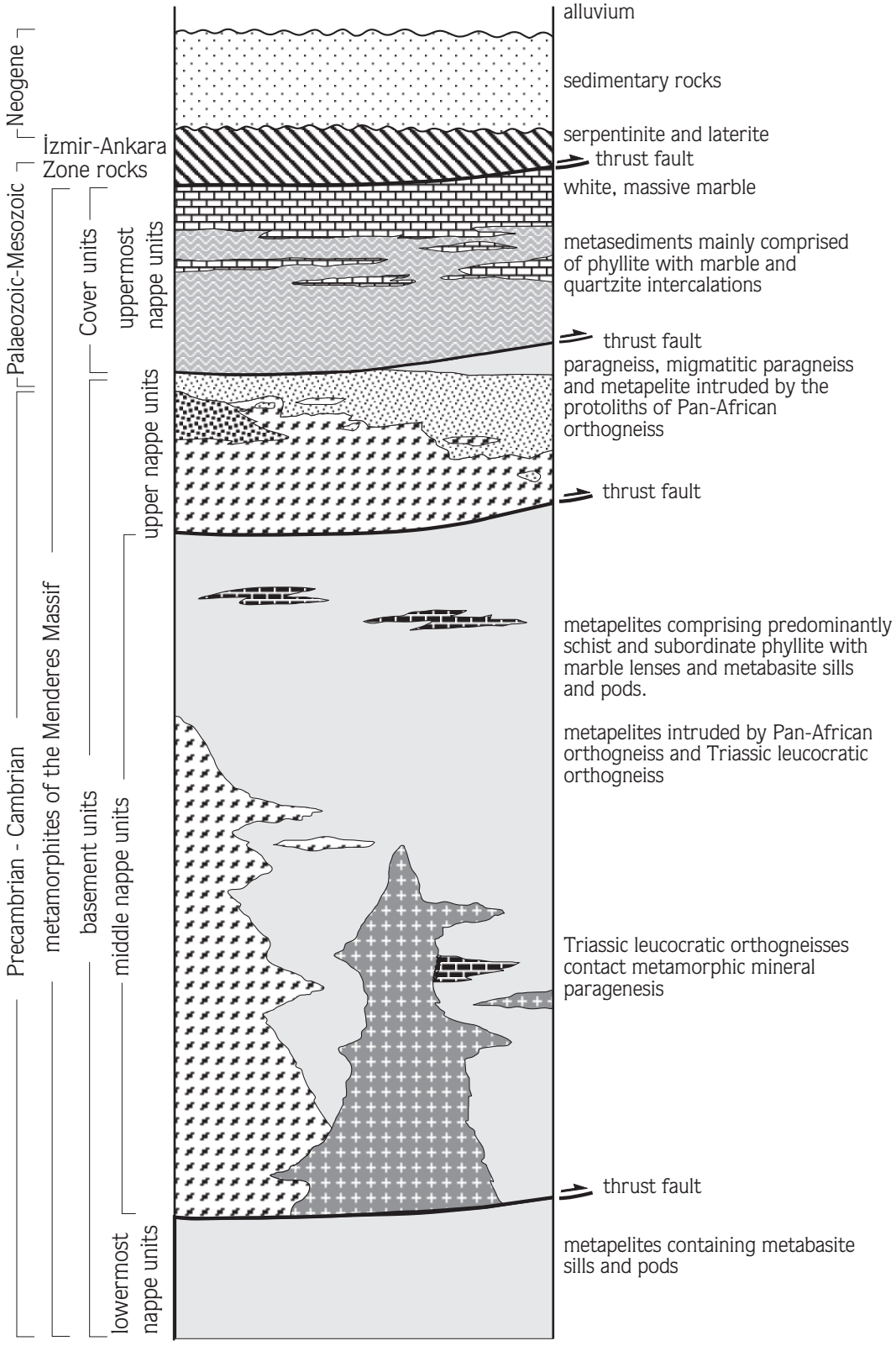

Figure 4. Generalised columnar section of the Derbent area.

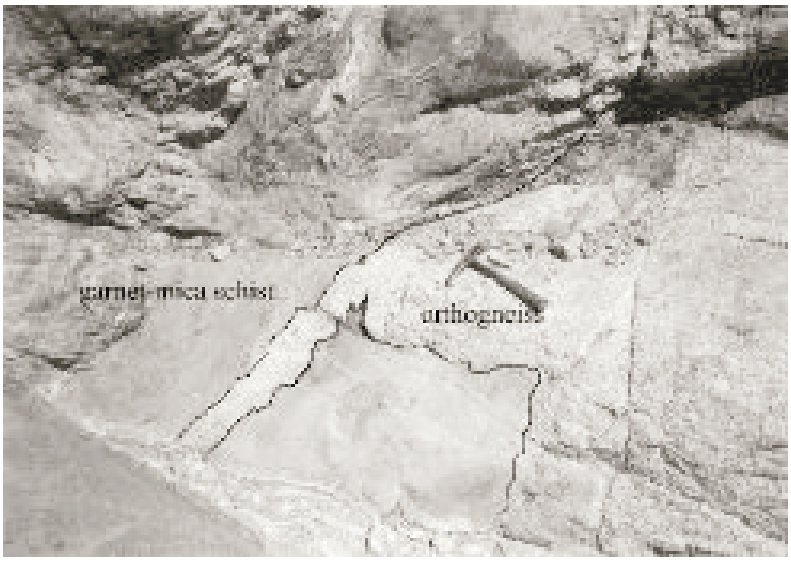

Figure 5. The contact relationship between orthogneiss and garnet-mica schist 2.5 km NE of Derbent. The boundary of orthogneiss cut across the main schistosity indicating the intrusive contact relationship. (Uşak L21-d1, 35500:29500). Hammer is 33-cm long.

Also, Rb–K_2O diagram exhibits low small data scatter and positive correlation. As for the trace elements, Ba and Zr show clear negative correlation with SiO_2, and Nb shows limited data spread and negative correlation, whereas Rb exhibits little spread and more-or-less constant values (Figure 6). This indicates that all these major and trace elements probably behaved in a less mobile way during metamorphism. On the other hand, Sr data separated into two groups on the diagram and lower values of Sr data show minor spread and more-or-less constant values, whereas Y exhibits broad data scatter indicative of substantial mobility.

On a Na_2O/Al_2O_3 versus K_2O/Al_2O_3 diagram (Figure 7a) the orthogneiss samples plot dominantly in the igneous field of Garrels & McKenzie (1971), with a few samples in the sedimentary field. An Al_2O_3 versus MgO diagram (Figure 7b), after Marc (1992), shows that the samples fall in the orthogneiss field. The chemical classification and nomenclature of volcanic rocks using the total alkali (Na_2O+K_2O) versus SiO_2 (TAS) diagram of Cox *et al.* (1979), adapted by Wilson (1989) for plutonic rocks, is used for the chemical classification and nomenclature of orthogneisses. The curved solid line divides the alkaline and sub-alkaline rocks. On this diagram, the orthogneisses lie within the granite field and show sub-alkaline affinity (Figure 8a). On the normative An–Ab–Or ternary diagram of Barker (1979), the rocks plot in the granite field (Figure 8b). Ti, Zr, Y and Nb are generally considered to be immobile during metamorphism (Winchester & Floyd 1977). On the SiO_2 versus Nb/Y and SiO_2 versus Zr/TiO_2 diagrams of Winchester & Floyd (1977), the samples fall predominantly into the granodiorite field (Figure 7c, d), with three samples that have relatively high SiO_2 content plotting in the granite field. In the Rb–Ba–Sr ternary diagram of El Bouseily & El Sokkary (1975), the samples plot on the boundary between the anomalous granite and normal granite fields (Figure 8e).

On the AFM ternary diagram with the dividing lines of Kuno (1968) and Irvine & Baragar (1971) to discriminate between tholeitic and calc-alkaline suites, the rocks follow a calc-alkaline trend (Figure 9a). The $Al_2O_3/(Na_2O+K_2O)$ versus $Al_2O_3/(CaO+Na_2O+K_2O)$ binary diagram has been used to discriminate peraluminous, metaluminous and peralkaline magma series (Shand 1943). This diagram reveals that the orthogneisses are peraluminous (Figure 9b), since the A/CNK ratio and normative corundum for the majority of the samples are greater than 1.5 and 1.0 wt% (Table 1), respectively.

The tectonic-setting discrimination diagrams based on trace elements, Nb versus SiO_2 (Figure 10a) and Rb

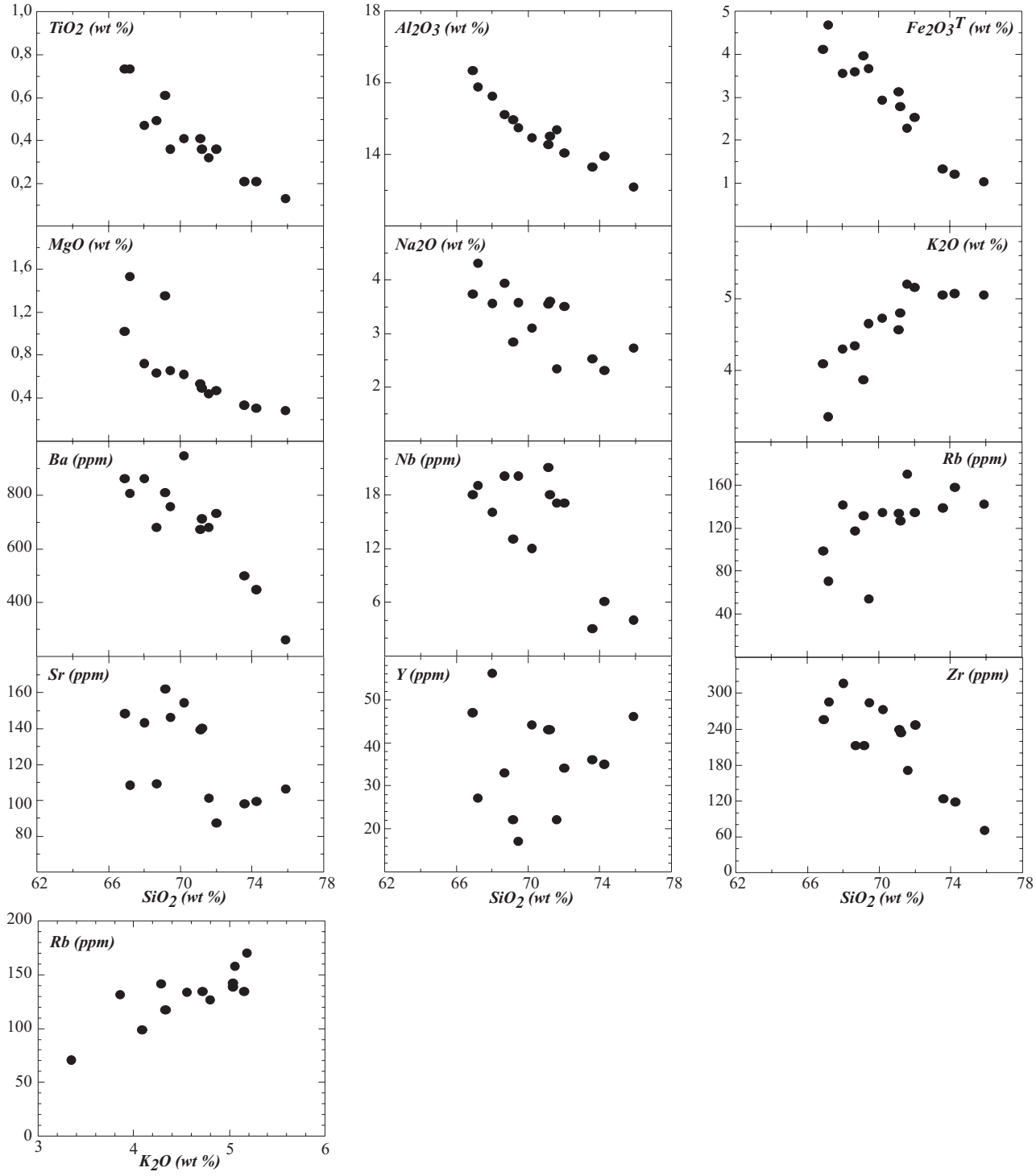

Figure 6. Harker variation diagrams for selected major and trace elements for the orthogneisses of the research area.

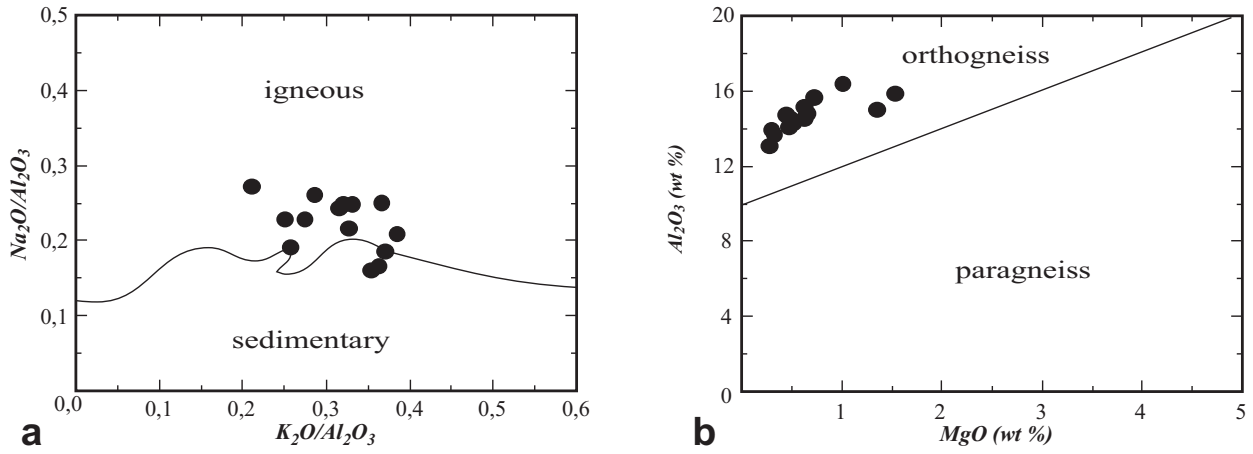

Figure 7. (a) Na_2O/Al_2O_3 vs K_2O/Al_2O_3 (after Garrels & McKenzie 1971); (b) Al_2O_3 vs MgO discrimination diagram (after Marc 1992).

versus Y+Nb (Figure 10b) (Pearce *et al.* 1984), show that our samples plot in the fields of VAG+COLG+ORG and Post-COLG, respectively. Batchelor & Bowden (1985) distinguished between the orogenic and non-orogenic plutons using R1 versus R2 parameters of the De la Roche *et al.* (1980). Most of the data points form a continuous trend from syn-collision to late orogenic field, very close to the post-orogenic field (Figure 10c). On the K_2O versus SiO_2 diagram of Coleman & Peterman (1975), all the samples plot in the granophyre field (Figure 10d), indicating that some crustal material was probably involved in their magma generation (Salem *et al.* 2001). Chappell & White (1974) used the $Al_2O_3/CaO+Na_2O+K_2O$ molecular ratio against normative corundum variation diagram to distinguish between I- (igneous) type (subduction related) and S-(sedimentary) type (collision related) granitic rocks. All of our points fall in the S-type granites field (Figure 10e).

Geochronology

Methods of the Single-Zircon $^{207}Pb/^{206}Pb$ Evaporation Technique

The selected representative zircons were separated at the Institute für Mineralogie, Petrologie und Geochemie, Eberhard-Karls Universität, Tübingen/Germany, using standard procedures. Only zircons without visible inclusions and with well-preserved crystal faces were selected, and only non-magnetic zircons were evaporated as these are usually less discordant than the others (Krogh 1982) and, therefore yield more accurate ages. The selected zircons typically were about 150 µm in width and 400 µm in length. Isotope measurements were carried out on a Finnigan MAT 262 mass spectrometer at the University of Tübingen. The zircons were dated using the single-zircon evaporation technique that measures the $^{207}Pb/^{206}Pb$ of evaporated crystals using a double Re-filament configuration. The principles of this method are described in Kober (1986, 1987), Kröner & Todt (1988) and Cocherie *et al.* (1992). Before use, all the Re-filaments were outgassed in a bake-out device for 30 minutes, using 5-A (0.7 mm-wide Re-filaments) and 6-A (1 mm filaments) currents. The outgassing was performed at a pressure close to 10^{-10} bar. One or more chemically untreated zircon grains were embedded in a 0.7 mm-wide canoe-shaped Re-filament, evaporation filament (Kober 1986), and first heated to evaporate Pb components with low activation energies. The evaporation filament was placed as close as possible to a second 1 mm-wide Re ionization filament. Data collection started at 1430 °C, and the temperature was increased stepwise by ca. 20 to 30 ºC after each evaporation and deposition cycle. The measurement of the isotopic abundance was performed in a dynamic mode with a mass sequence 206–207–204–206–207 or 206–207–207–206–204 using an ion-counter. The ages were calculated from the $^{207}Pb/^{206}Pb$ ratios obtained on a stable ion beam, and only ratios with $^{206}Pb/^{204}Pb$ ratios > 5000 were used for further processing. A correction for common Pb was performed according to Cocherie *et al.*

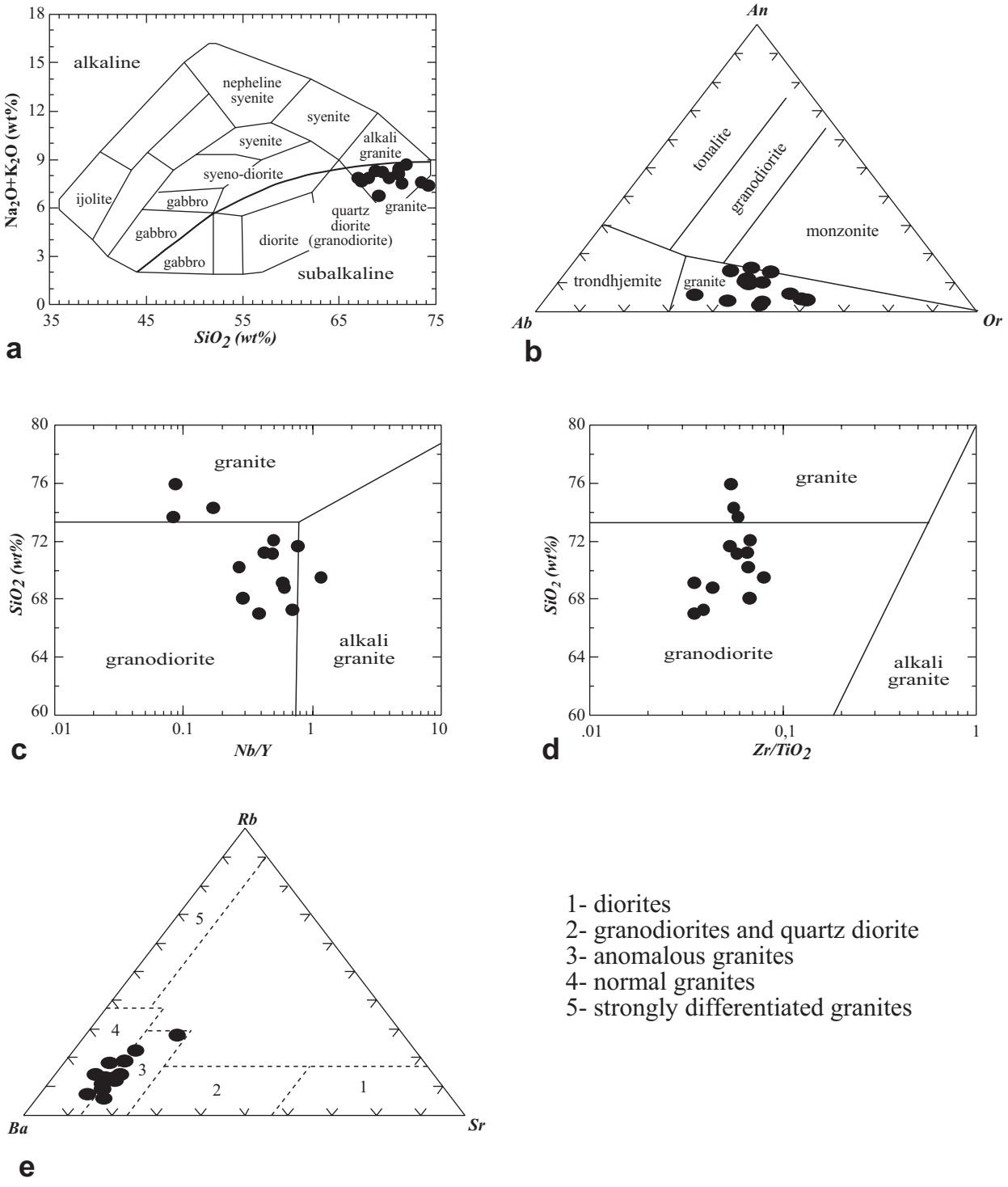

Figure 8. (a) Chemical classification and nomenclature of plutonic rocks using the total alkalis (Na_2O+K_2O) vs SiO_2 (TAS) diagram of Cox *et al.* (1979), adapted by Wilson (1989) for plutonic rocks; (b) normative An-Ab-Or diagram for the granitoids (Barker 1979); classification of the protoliths of the orthogneisses on (c) SiO_2 vs Nb/Y and (d) SiO_2 vs Zr/TiO_2 binary plots (adapted from Winchester & Floyd 1977); (e) Ba–Sr–Rb diagram of El Bouseily & El Sokkary (1975).

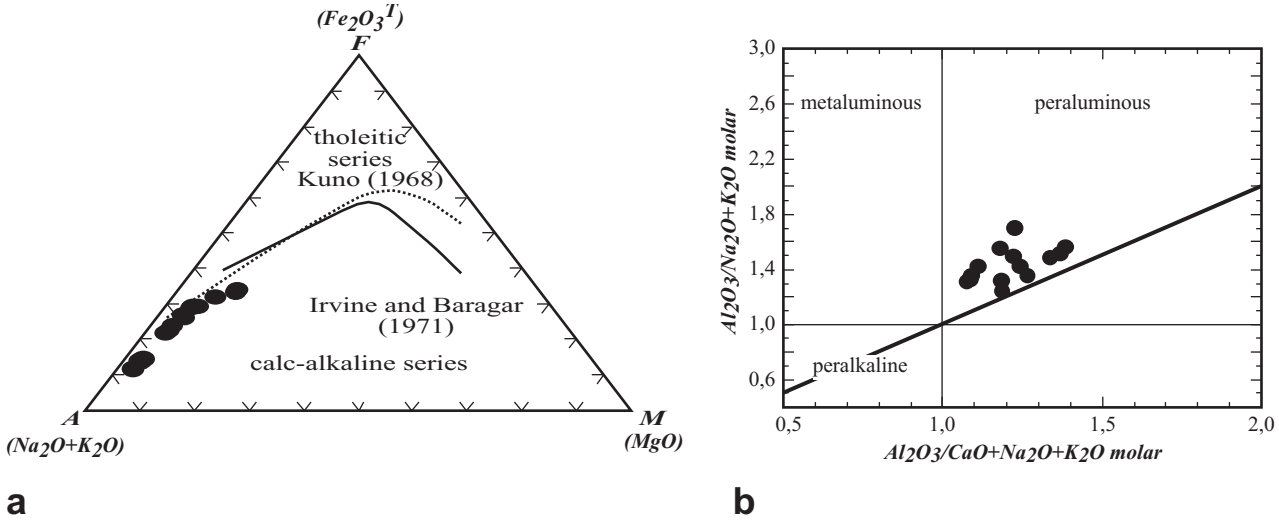

Figure 9. (a) AFM ternary diagram with the dividing lines after Kuno (1968) and Irvine & Baragar (1971); (b) Shand's index; $Al_2O_3/(Na_2O+K_2O)$ vs $Al_2O_3/(CaO+Na_2O+K_2O)$ binary plot for the granitic protolith (after Maniar & Piccoli 1989).

(1992) using a Pb composition with a two-stage evolution (Stacey & Kramers 1975). Measurements of the Pb standard NBS 981 in ion-counting mode yielded an average fractionation of ca. 0.1% per atomic mass unit (Chen *et al.* 2000). This value is considered a suitable estimate for correction of mass fractionation. The errors on the ages are reported as $2\sigma_{mean}$ of the population of weighted $^{207}Pb/^{206}Pb$ ratios (Table 2).

Zircon Morphology

Zircons from three orthogneiss samples were investigated under the scanning electron microscope (SEM) (Figure 11). Twenty crystals were chosen from each zircon type for typological investigation (Pupin 1980) by SEM. The zircon concentrates were studied optically and divided into individual types. Selection for analysis was based on differences in size, colour, morphology, inclusions, turbidity, abundance of cores, lack of cracks, etc. In samples 95–57, 96–34 and 97–58, all zircons had similar morphologies which were typical of magmatic zircons (Figure 11). They are euhedral, sometimes asymmetric, colourless to slightly pink and brown, transparent, clear to slightly turbid, short- (2:1) and long- (3:1, 4:1) prismatic, occasionally metamict, and have few inclusions. According to the classification of Pupin & Turco (1974), these zircons predominantly belong to subtypes S7 and S12 and, to a lesser extent, to subtypes L1, S17, S13, and S2 (Figure 12). In other words, the zircons of these orthogneisses are characterised by a combination of (101) < (211)-pyramids and (100) < (110) and (100) = (110)-prisms (Figure 12). The crystallisation temperatures of the predominant subtypes is estimated at 700–750 °C (Pupin & Turco 1974). The typological analysis of the zircon populations places them in the field of intrusive, peraluminous, crustal-derived granites (Pupin 1980).

The cathodoluminescence (CL) technique, allowing an examination of magmatic zoning, inherited cores and overgrowth in zircon grains, was used for investigating the internal structures of the zircons. The zircons of our samples are similar to each other with respect to internal structures of the cores and zoned overgrowths. Most of the elongated prismatic zircons have no cores and show typical oscillatory zoning, indicative of a magmatic origin (Figure 13a–c, f–h). These types of grains were selected for evaporation analyses. Some zircon grains contain inherited (detrital) cores of highly variable size and multiple growth stages (Figure 13d, e, i, j) (not analysed). Primary older growth zoning is well preserved in parts of some cores (Figure 13d, j) whereas, in others, it is largely obliterated and apparently replaced by strongly luminescent and nearly homogenous stubby zircon. The cores and overgrowths are separated by well-preserved

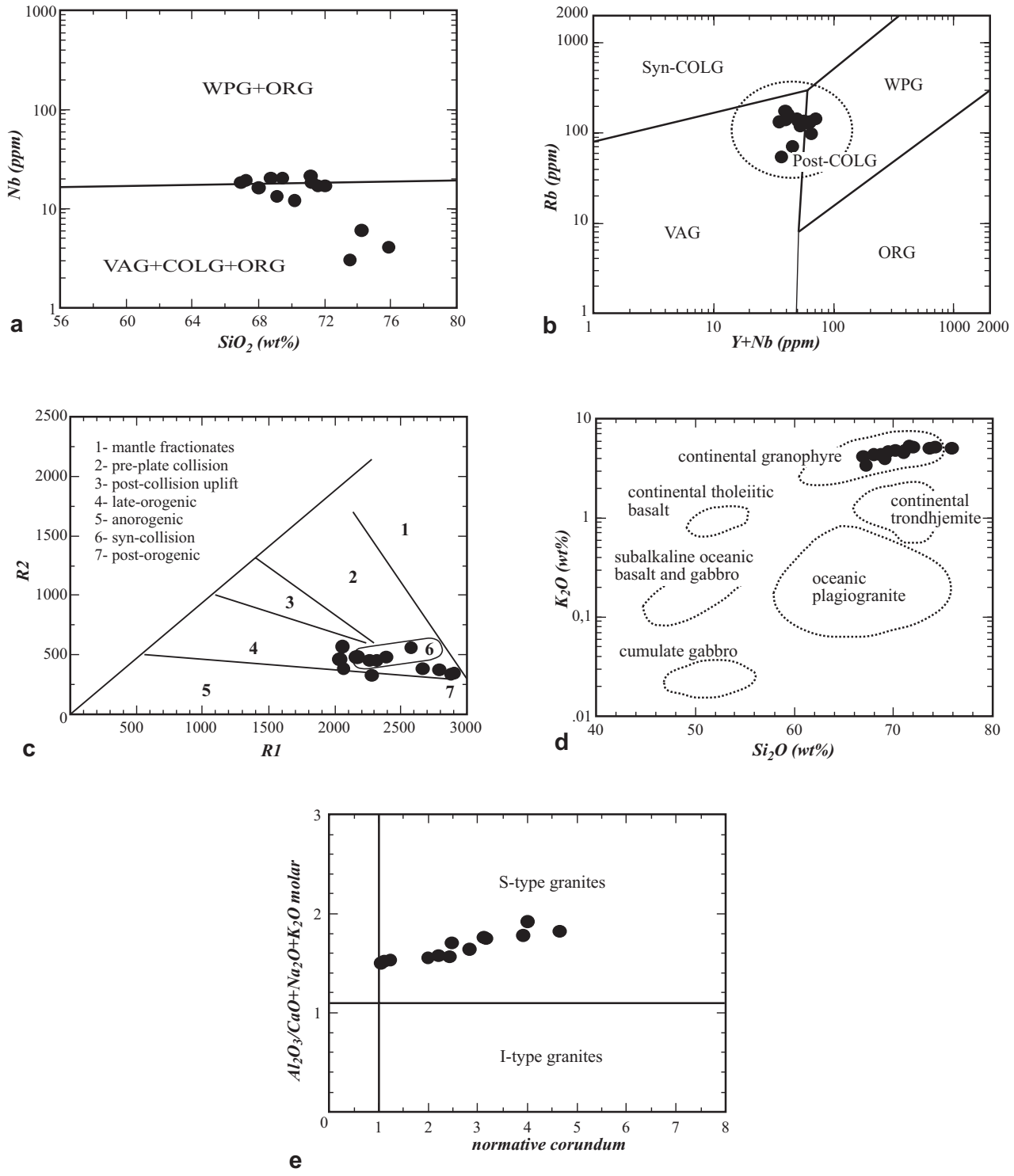

Figure 10. SiO_2 variation diagrams for tectonic discrimination of the protolith of the augen/granitic gneisses; **(a)** Nb vs SiO_2; and **(b)** Rb vs Y+Nb (after Pearce *et al.* 1984). ORG: ocean-ridge granitoids; syn-COLG: syn-collisional granitoids; COLG: collisional granitoids; VAG: volcanic-arc granitoids; WPG: within-plate granitoids; **(c)** R1-R2 multicationic diagram (after De la Roche *et al.* 1980); **(d)** K_2O vs SiO_2 diagram (after Coleman & Peterman 1975); **(e)** Normative corundum vs molar A/CNK binary plot (field boundaries are from Chappell & White (1974).

Table 2. Radiogenic $^{207}Pb/^{206}Pb$ ratios of evaporated zircon grains and corresponding ages.

Sample number	Zircon description	Grain	Number of ratio	Evaporation temperature (°C)	$^{207}Pb/^{206}Pb$ ratios (mean)	$^{207}Pb/^{206}Pb$ Age (Ma)
96–34	cl, c, t, lp	1	129	1460–1490	0.058564±50	561.5±1.9
	cl, c, t, lp	2	88	1460–1480	0.058942±33	564.5±1.2
	cl, c, t, lp	3	57	1520	0.058866±24	561.6±0.9
	y, c, t, lp	4	208	1450–1490	0.058592±43	551.4±1.9
	Mean (grain 1,2,3,4)		482		0.058564±22	561.5±0.8 (2σm)
97–58	p, c, t, lp	1	51	1530	0.063375±31	720.3±1.1
	cl, c, t, lp	2	75	1540	0.059326±92	578.5±3.4
	cl, c, t, lp	3	52	1540	0.059012±39	567.0±1.4
	cl, c, t, lp	4	17	1450	0.58678±209	554.6±7.8
	Mean (grain 2,3,4)		144		0.059125±62	570.5±2.2 (2σm)

p - pink, y - yellowish, cl – colourless, c – clear, t – translucent, lp - long prismatic

resorption surfaces marked by 'C' in Figure 13 (d, e, i and j). This complex zircon population provides evidence for the protoliths of orthogneisses that are of hybrid granitoids with mostly S-type components or S-type rock (Poller 1999).

Description of the Samples and $^{207}Pb/^{206}Pb$ Ages

Two samples (96–34 and 97–58) from different orthogneiss bodies were selected for $^{207}Pb/^{206}Pb$ isotopic dating (Figure 3).

Sample 96–34 was collected 1.5 km east of Aksu village (Figure 3). The rock is composed of quartz, orthoclase, plagioclase, muscovite, biotite, zircon, apatite and opaque oxides. The zircon grains are predominantly white, yellowish, light pink, clear, translucent and short- and long-prismatic. SEM images show that the zircon grains are euhedral, and have morphologies which strongly suggest an igneous origin (Figure 11). The zircon grains were inspected with CL for evidence of magmatic zonation, inherited zircons, and new overgrowth. Most of the zircons are predominantly long-prismatic and perfectly euhedral. They show oscillatory zoning indicating a magmatic origin (Figure 13a–c). The CL photographs indicate multiple growth stages (Figure 13b) and xenocrystic cores with oscillatory zoning for some zircon crystals (Figure 13d, e). Four long-prismatic grains (Figure 13a–c) from this sample were evaporated individually and yielded ages of 550 to 564 Ma. An average value of 561.5±1.8 Ma was obtained (Table 2, Figure 14a). This age is interpreted to represent the intrusion age of the magmatic protoliths of the orthogneiss.

Sample 97–58 was collected 2 km southwest of Bahadır village (Figure 3). It shows well-developed schistosity and comprises quartz, orthoclase, plagioclase, muscovite, biotite, zircon, apatite, tourmaline and opaque oxides. The zircon grains are predominantly white, pink, clear, translucent and short- and long-prismatic. SEM photographs show that the zircons are euhedral, and have morphologies that point to an igneous origin (Figure 11). A CL study revealed magmatic zonation, inherited zircons, and new overgrowth. The zircons are predominantly long-prismatic and euhedral - typical of granitic populations (Figure 13f–h). Some zircon grains have xenocrystic cores (Figure 13i, j) and preserve oscillatory zoning of magmatic origin. The CL images indicate multiple growth stages for some zircon crystals (Figure 13g, h). Four long-prismatic grains (Figure 13f–h) of this sample were evaporated and yielded ages of 520 to 720 Ma. Three grains of this sample yielded an average value of 570.5±2.2 Ma (Table 2, Figure 14b). This age is interpreted as the intrusion age of the magmatic protolith of the orthogneiss. In this sample, an older zircon grain yielded age of 720.3±1.1 Ma, which is interpreted as an inherited grain (Table 2).

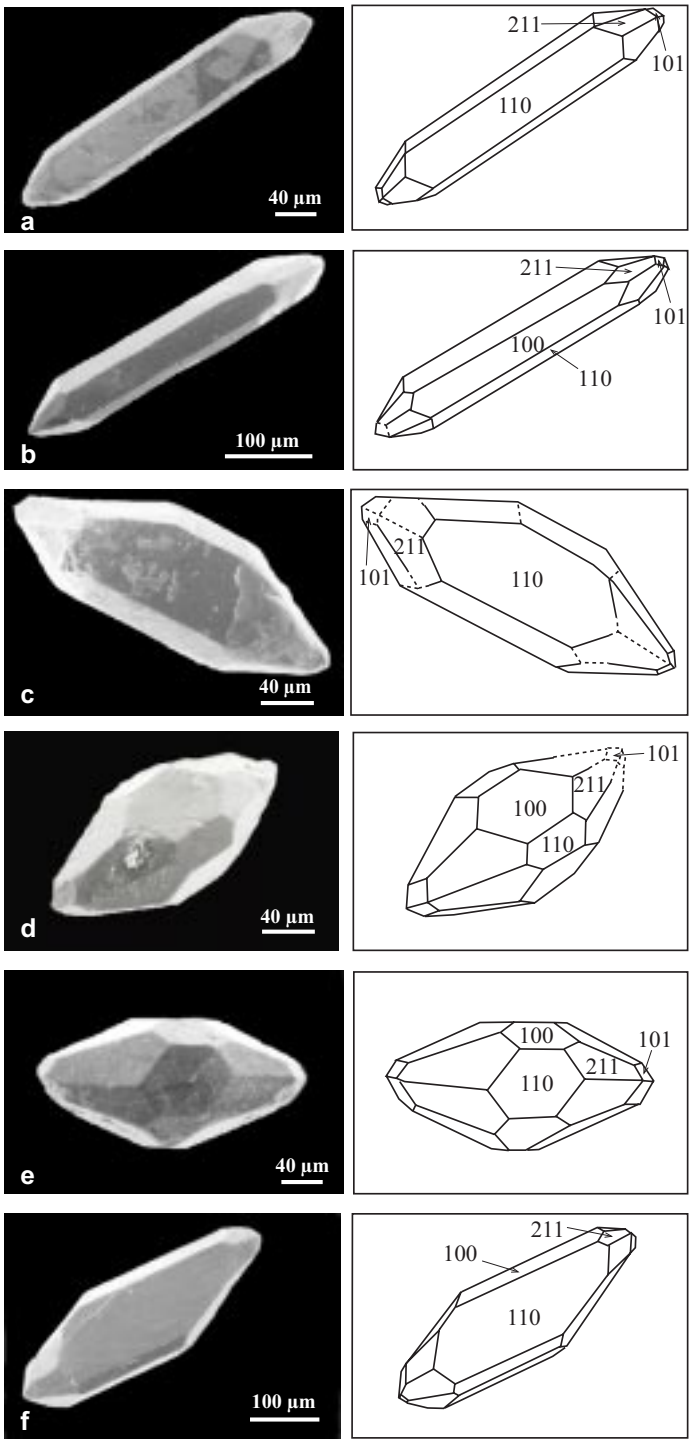

Figure 11. SEM images of typical zircons from the orthogneisses. (a) clear, colourless, long-prismatic, clustering around L1; (b) clear, colourless, long-prismatic, clustering around S12; (c) clear, colourless and slightly pink, long-prismatic, clustering around S7; (d) clear, colourless and slightly pink, long-prismatic clustering around S17; (e) clear, colourless, slightly pink and brown, short and long-prismatic, clustering around S7; (f) clear, colourless, long-prismatic, clustering around S2.

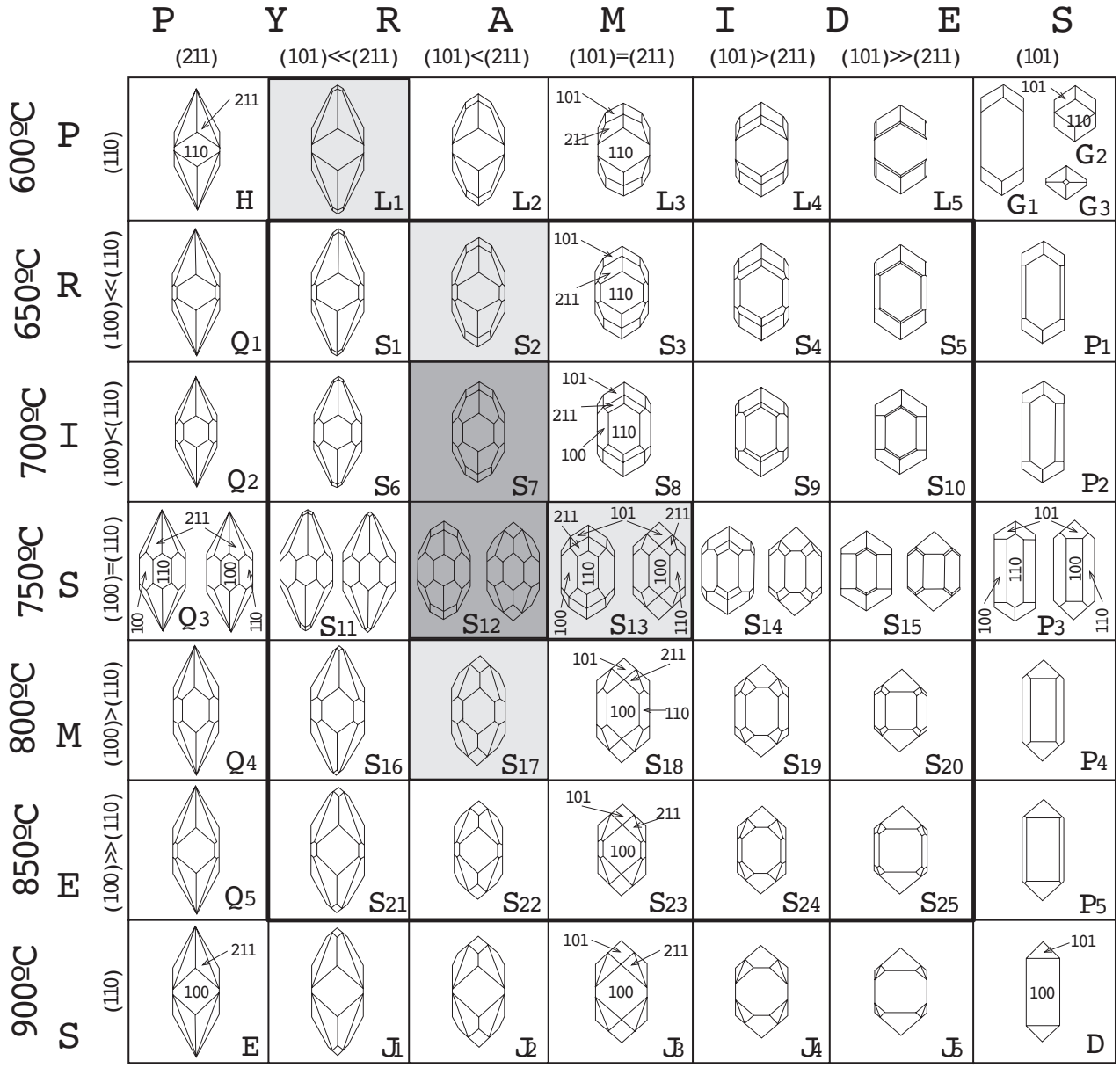

Figure 12. Main types and subtypes of the typologic classification and corresponding geothermometric scale, after Pupin & Turco (1972).

Discussion

The overall aim of this study was to understand constraints on the Pan-African geological evolution of the orthogneisses of the basement rocks in the Ödemiş-Kiraz submassif of the Menderes Massif (western Turkey). The origin of these orthogneisses has been controversial for many years. Especially in previous studies, most researchers suggested sedimentary protoliths for these orthogneisses (Schuiling 1962; Başarır 1970, 1975; Akat *et al.* 1975; Akdeniz & Konak 1979; Öztürk & Koçyiğit 1983; Akkök 1983; Akkök *et al.* 1984; Şengör *et al.* 1984; Satır & Friedrichsen 1986). Öztürk & Koçyiğit (1983) proposed a sedimentary origin due to the intercalation of orthogneisses with quartz arenites which

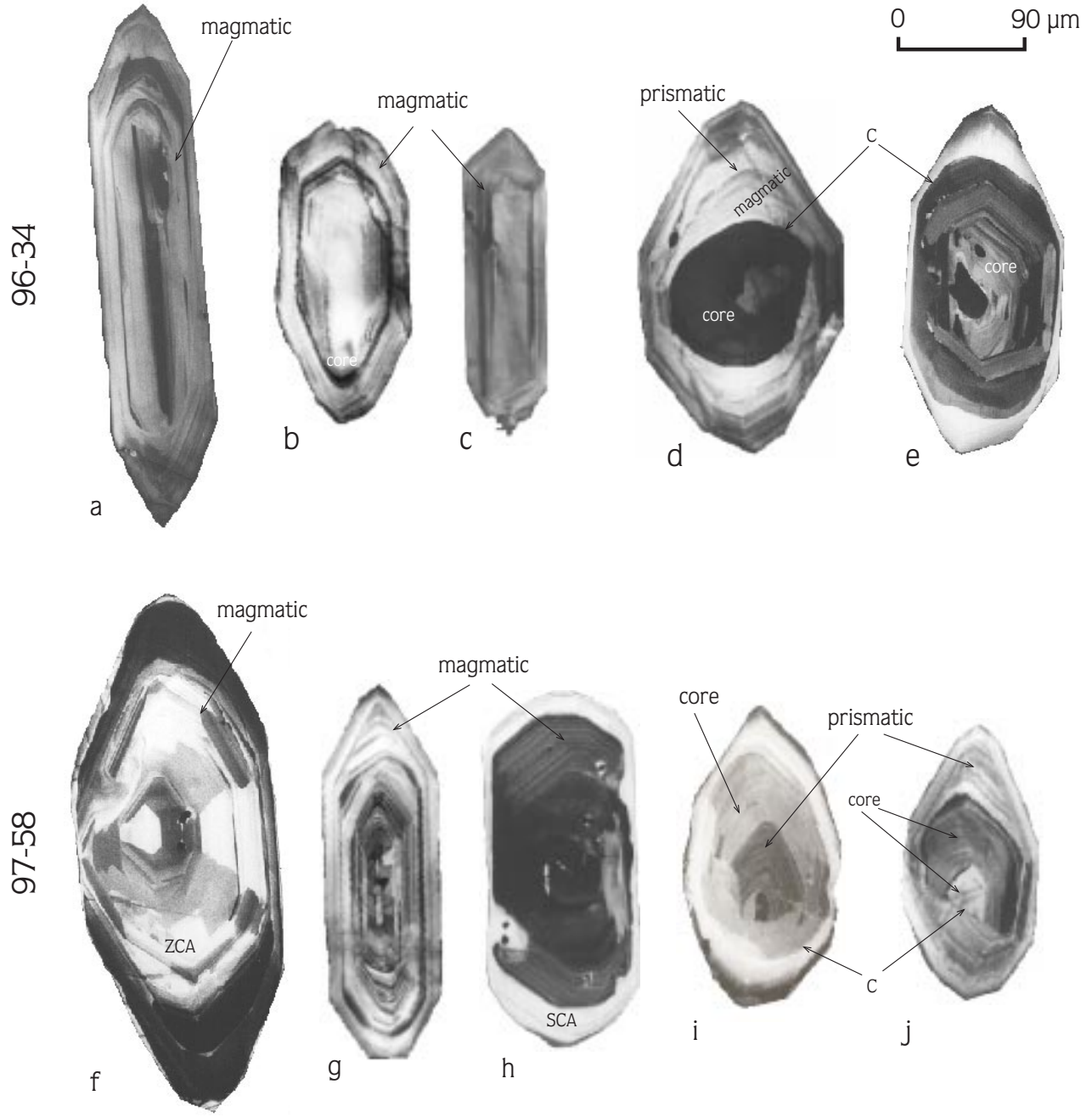

Figure 13. Cathodoluminescence (CL) images of characteristic zircon populations in the orthogneisses. A characteristic feature of the zircons is oscillatory zoning indicating a magmatic origin **(a–c, f–h)**. Zircons with older core are shown in d, e, i and j. ZCA– zoning-controlled alteration, SCA– surface-controlled alteration, C– the sharp boundary (resorption surface) between cores and overgrowths.

show some features interpreted as primary cross-bedding. Ages scattered between 545 and 670 Ma, based on an Rb/Sr whole rock isochron age, were interpreted as the sedimentation ages of the protoliths of the gneisses by Satır & Friedrichsen (1986). Alternatively, a granitic protolith has been suggested by some researchers (Graciansky 1965; Konak 1985; Konak *et al.* 1987; Erdoğan 1992, 1993; Bozkurt 1994; Bozkurt & Park

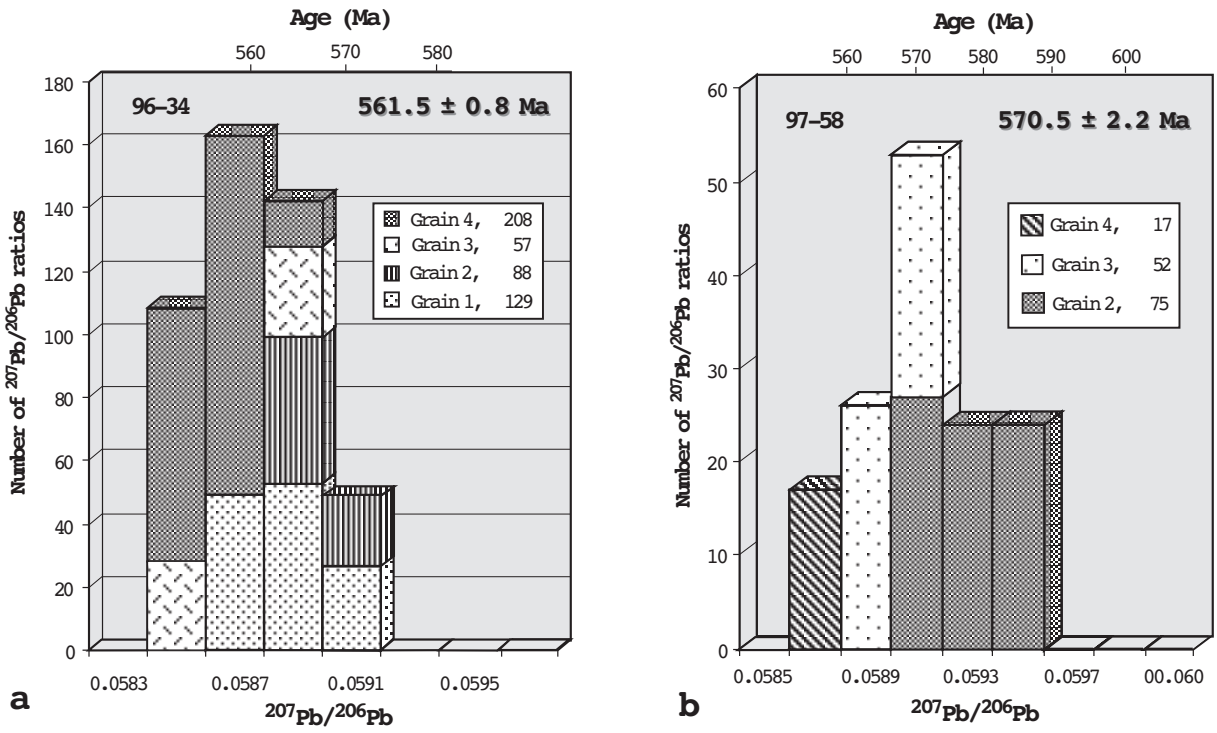

Figure 14. Zircon ages for orthogneiss samples, 96–34 and 97–58. Histograms of radiogenic $^{207}Pb/^{206}Pb$ ratios for evaporated zircons indicating ages of 561.5±0.8 Ma ($2\sigma_{mean}$) and 570.5±2.2 Ma ($2\sigma_{mean}$), respectively.

1994, 1997a, 1997b, 1999, 2001; Bozkurt *et al.* 1992, 1993, 1995; Mittwede *et al.* 1995a, 1995b, 1997; Hetzel & Reischmann 1996; Loos & Reischmann 1999). This suggestion was based mainly on: (i) the weathering style (spheroidal weathering) and morphological features (bald hills) (Bozkurt 1994); (ii) petrographic characteristics and field relations (preserved primary intrusive contact relationships between orthogneisses and predominantly metasedimentary country rocks) (Erdoğan 1992, 1993; Bozkurt *et al.* 1992, 1993, 1995; Mittwede *et al.* 1995a, 1995b, 1997) and the geochemical characteristics of orthogneisses (Bozkurt *et al.* 1992, 1993, 1995; Mittwede *et al.* 1995a, 1995b, 1997). Konak *et al.* (1987) and Dora *et al.* (1990) have drawn a distinction between the augen and granitic gneisses. According to these authors, while the augen gneisses have a distinct sedimentary origin, the granitic gneisses were derived from a granitic precursor. Dora *et al.* (1994) suggested that the protoliths of all gneisses (with different structures) are syn- to post-metamorphic granites which intruded the basement during the last stage of the Pan-African Orogeny. Based on their geochemical characteristics, the protoliths of the augen gneisses have been interpreted as calc-alkaline, peraluminous, S-type, syn- to post-tectonic granites and granodiorites (Bozkurt *et al.* 1992, 1993, 1995; Dannat 1997; Koralay & Dora 1999).

The orthogneisses exposed in the study area (eastern part of the Ödemiş-Kiraz submassif) have well-preserved, original intrusive contact relationships with Precambrian country rocks (Figure 5), clearly revealing the igneous origin of these rocks. In this study, geochemical analyses show that the orthogneisses are of similarly igneous origin and have a granitic to granodioritic composition. They originated from S-type, peraluminous, calc-alkaline magma involving some crustal material, and these rocks have geochemical signatures indicative of a syn- to post-collisional tectonic environment.

In previous studies, Rb–Sr age determinations done on whole-rock orthogneiss samples from the Çine submassif yielded isochron ages of 490±90 Ma (Dora 1975, 1976) and 471±9 Ma (Şengör *et al.* 1984; Satır

& Friedrichsen 1986) which were interpreted as intrusion ages of the protoliths. Most of the recent geochronological studies were carried out on orthogneisses in the Çine submassif, southern submassif of the Menderes Massif. Hetzel & Reischmann (1996) proposed that 546.2±1.2 Ma is interpreted as the intrusion age of the granitic precursor of the augen gneisses in the southern Menderes Massif. Loos & Reischmann (1999) have obtained 521±8 Ma to 572±7 Ma intrusion ages from augen gneiss samples north of Selimiye in the Çine submassif (southern Menderes Massif). Similar intrusion ages, 547±1 Ma and 566±9 Ma, have already been reported in various parts of the Çine submassif by Gessner *et al.* (2001b) and Gessner *et al.* (2004), respectively. These data were obtained from zircons using the $^{207}Pb/^{206}Pb$ single-grain evaporation and SHRIMP methods. In the Ödemiş-Kiraz submassif, very limited geochronological studies have been done on the orthogneisses. Dannat (1997) has interpreted that the age of 528.0±4.3 Ma is the intrusion age of augen gneisses that cut paragneisses of upper nappe unit in the Derbent area (Figure 3). An anatectic metagranite derived from paragneisses from the Ödemiş-Kiraz submassif, dated by the conventional U–Pb method, yielded an intrusion age of 551.5±1.4 Ma (Hetzel *et al.* 1998). All these ages cluster between 540 Ma and 550 Ma and demonstrate that large volumes of orthogneiss in the Menderes Massif are the result of magmatic activity related with to the Pan-African Orogeny (Şengör *et al.* 1984; Kröner & Şengör 1990; Dora *et al.* 1990; Hetzel & Reischmann 1996; Dannat & Reischmann 1997; Loos & Reischmann 1999).

In the study area, first-time investigations of zircon grains from orthogneisses intruding the Precambrian schist of the middle nappe unit yield ages of 561.5±1.8 Ma and 570.5±2.2 Ma. These Pb–Pb ages are interpreted as the intrusion age of the protoliths of the orthogneisses. As SEM- and CL-photographs (Figures 11 & 13) demonstrate, the analysis of zircon populations shows distinct magmatic zonation and typical igneous characteristics. One grain of the idiomorphic variety of sample 97–58 was analysed and yielded a distinctly higher isotopic ratio from which an age of 720.3±1.1 Ma was calculated (Table 2). This grain most likely represents a xenocryst from an older source that contaminated the protoliths of the orthogneiss during its formation and/or ascent, as indicated in the geochemistry section above. Similar zircon ages (719–721 Ma; Koralay *et al.* 2003) were reported from paragneisses, interpreted as the most probable source rock for the protolith of the orthogneisses in the Menderes Massif.

Dalziel (1997) and Hofmann (1991) suggested that the Pan-African and Brazilide ocean basins within the amalgamating cratons of Gondwana were closing during the Neoproterozoic until, at least, Cambrian time. Closure of several Pan-African – Brazilide ocean basins resulted in the amalgamation of East and West Gondwana (Stern 1994; Trompette 1994; Stein & Goldstein 1996; Unrug 1996). The collision with Arabian terranes constituted Gondwanaland and wrench faulting, granite plutonism and molasse sedimentation occurred during the 630–530 Ma interval (Piper 2000). Şengör *et al.* (1984) emphasise, based on an age of about 500±10 Ma – interpreted to represent the deformation and metamorphism of the core series of the Menderes Massif – that the metamorphism of the Precambrian basement was related to the Pan-African Orogeny. The granitic precursors of orthogneisses, dated at 560 Ma and 570 Ma, are regarded to have been related to magmatic activity subsequent to the Pan-African Orogeny (Dora *et al.* 1994, 1995; Hetzel & Reischmann 1996; Dannat & Reischmann 1998; Hetzel *et al.* 1998; Koralay & Dora 1999). The same common magmatic activities are documented all over Africa (Stern 1994; Kröner *et al.* 1991, 1996; Tack & Bowden 1999; Hefferan *et al.* 2000; Jung *et al.* 2000) and were reported in NNE Africa as forming a part of West Gondwana (Kröner *et al.* 1983; Tadese *et al.* 2000; Teklay *et al.* 1998, 2001; Moghazi 2002). This evidence, when combined with reconstruction of the continents at the Late Neoproterozoic–Cambrian boundary, indicates that the Pan-African basement of the Menderes Massif formed as a part of West Gondwana (NNE Africa) during the Pan-African Orogeny. Syn- to post- Pan-African magmatism, which is characterised by granitoid intrusions, is commonly recognised in this orogenic belt and also in the Menderes Massif.

Conclusions

1. The precursor rocks of the orthogneisses intruded the protoliths of the Pan-African basement series, which consists of metapelites. Numerous sills and dykes of orthogneiss, which clearly crosscut the schistosity of

the schists and have sharp contacts, are found in the schists close to the margins of orthogneiss. The orthogneisses contain numerous schist xenoliths which are particularly common close to contacts. The abundance of xenoliths in the orthogneisses and the veins in the country rock clearly reveal the original intrusive contact relationship between the orthogneiss and metapelites.

2. The geochemical data indicate that the protoliths of the Pan-African orthogneisses were calc-alkaline, peraluminous and S-type, and generated in a syn- to post-tectonic environment.
3. The SEM and CL photomicrographs demonstrate that the analysed zircon populations from the orthogneisses have distinct magmatic zoning and typical igneous morphology. The $^{207}Pb/^{206}Pb$ ages of 561.5±1.8 and 570.5±2.2 Ma are interpreted as the intrusion ages of the protoliths of the Pan-African orthogneisses.
4. Widespread magmatic activity at around 520–570 Ma in the Menderes Massif can be interpreted as representing the effects of the Pan-African Orogeny, which was related to closure of the Pan-African and Brazilide ocean basins and amalgamation of East and West Gondwana.

Acknowledgements

E. Koralay is grateful for the German Academic Exchange Service (DAAD) scholarship to undertake this research at the University of Tübingen. We thank G. Bartholomä, M. Schuman and B. Steinhilber for the XRF analyses at Tübingen. The authors are grateful to S. Mittwede and H. Yılmaz for critically reading the manuscript. R. Oberhänsli and an anonymous referee are thanked for their useful and constructive comments. This paper forms a part of a Ph.D. study carried out by E. Koralay under the supervision of O.Ö. Dora.

References

AKAT, U., ÖZTÜRK, Z., ÖZTÜRK, E. & ÇAĞLAYAN, A. 1975. *Menderes Masifi Güneyi – GB Toros Kuşağı İlişkisi [Relationship Between the Southern Menderes Massif and the SW Taurus Belt]*. General Directorate of Mineral Research and Exploration Institute of Turkey (MTA), Project No: **5488** [in Turkish, unpublished].

AKDENİZ, N. & KONAK, N. 1979. Menderes Masifi'nin Simav dolaylarındaki kaya birimleri ve metabazik, metaultramafik kayaların konumu. [Rocks of the Menderes Massif around Simav and the significance of metabasic and meta-ultrabasic rocks] *Geogical Society of Turkey Bulletin* **22**, 175–183 [in Turkish with English abstract].

AKKÖK, R. 1983. Structural and metamorphic evolution of the northern part of the Menderes Massif: New data from the Derbent area and their implication for the tectonics of the massif. *Journal of Geology* **91**, 342–350.

AKKÖK, R., SATIR, M. & ŞENGÖR, A.M.C. 1984. Menderes Masifi'nde tektonik olayların zamanlaması ve sonuçları [Timing of tectonic events in the Menderes Massif and its significance]. *Ketin Symposium, Abstracts,* 93–94.

BARKER, F. 1979. Trondhjemites: definition, environment and hypothesis of origin. *In*: BARKER F. (ed), *Trondjemites, Dacites and Related Rocks*. Elsevier, 1–12.

BAŞARIR, E. 1970. *Bafa Gölünün Doğusunda Kalan Menderes Masifi Güney Kanadının Jeolojisi ve Petrografisi [Geology and Petrography of the Southern Sector of the Menderes Massif to the East of Lake Bafa]*. Faculty of Science Publication, Ege University **102**.

BAŞARIR, E. 1975. *Çine Güneyindeki Metamorfitlerin Petrografisi ve Bireysel İndeks Minerallerin Doku İçerisindeki Gelişimleri [The Petrography of the Metamorphics Exposed to the South of Çine and the Growth of Individual Index Minerals within the Metamorphic Texture]* DSc Thesis, Ege University, İzmir.

BATCHELOR, R.A. & BOWDEN, P. 1985. Petrogenetic interpretation of granitoid rock series using multicationic parameters. *Chemical Geology* **48**, 43–55.

BOZKURT, E. 1994. *Effects of Tertiary Extension in the Southern Menderes Massif, Western Turkey*. PhD Thesis, University of Keele.

BOZKURT, E. 1996. Metamorphism of Palaeozoic schists in the southern Menderes Massif: field, petrographic, textural and microstructural evidence. *Turkish Journal of Earth Sciences* **5**, 105–121.

BOZKURT, E. 2000. Timing of Extension on the Büyük Menderes Graben, Western Turkey and its tectonic implications. *In*: BOZKURT, E., WINCHESTER, J.A. & PIPER, J.D.A. (eds), *Tectonics and Magmatism in Turkey and the Surrounding Area.* Geological Society, London, Special Publication **173**, 385–403.

BOZKURT, E. 2001a. Neotectonics of Turkey – a synthesis. *Geodinamica Acta* **14**, 3–30.

BOZKURT, E. 2001b. Late Alpine evolution of the central Menderes Massif, western Anatolia, Turkey. *International Journal of Earth Sciences* **89**, 728–744.

BOZKURT, E. 2002. Discussion on the extensional folding in the Alaşehir (Gediz) Graben, western Turkey. *Journal of the Geological Society, London* **159**, 105–109.

BOZKURT, E. 2003. Origin of NE–trending basins in western Turkey. *Geodinamica Acta* **16**, 61–81.

BOZKURT, E. & OBERHÄNSLI, R. 2001. Menderes Massif (western Turkey): structural, metamorphic and magmatic evolution – a synthesis. *International Journal of Earth Sciences* **89**, 679–708.

BOZKURT, E. & PARK, R.G. 1994. Southern Menderes Massif: an incipient metamorphic core complex in western Anatolia, Turkey. *Journal of the Geological Society, London* **151**, 213–16.

BOZKURT, E. & PARK, R.G. 1997a. Evolution of a mid-Tertiary extensional shear zone in the southern Menderes Massif, western Turkey. *Societe Geologique de France Bulletin* **168**, 3–14.

BOZKURT, E. & PARK, R.G. 1997b. Microstructures of deformed grains in the augen gneisses of southern Menderes Massif and their tectonic significance. *Geologische Rundschau* **86**, 103–119.

BOZKURT, E. & PARK, R.G. 1999. The structure of the Palaeozoic schists in the southern Menderes Massif, western Turkey: a new approach to the origin of the main Menderes metamorphism and its relation to the Lycian Nappes. *Geodinamica Acta* **12**, 25–42.

BOZKURT, E. & PARK, R.G. 2001. Discussion on the evolution of the southern Menderes Massif in SW Turkey as revealed by zircon dating. *Journal of the Geological Society, London* **158**, 393–395.

BOZKURT, E. & SATIR, M. 2000. The southern Menderes Massif (western Turkey): geochronology and exhumation history. *Geological Journal* **35**, 285–296.

BOZKURT, E. & SÖZBILIR, H. 2004. Tectonic evolution of the Gediz Graben: field evidence for an episodic, two-stage extension in western Turkey. *Geological Magazine* **141**, 63–79.

BOZKURT, E., PARK, R.G. & WINCHESTER, J.A. 1992. Evidence against the core/cover concept in the southern sector of the Menderes Massif. *Turkish Geology Workshop (Work in Progress on the Geology of Turkiye), 9–10 April, Keele*, p. 22.

BOZKURT, E., PARK, R.G. & WINCHESTER, J.A. 1993. Evidence against the core/cover interpretation of the southern sector of the Menderes Massif, west Turkey. *Terra Nova* **5**, 445–451.

BOZKURT, E., WINCHESTER, J.A. & PARK, R.G. 1995. Geochemistry and tectonic significance of augen gneisses from the southern Menderes Massif (West Turkey). *Geological Magazine* **132**, 287–301.

ÇAĞLAYAN, M.A., ÖZTÜRK, E.M., ÖZTÜRK, Z., SAV, H., & AKAT, U. 1980. Menderes Masifi güneyine ait bulgular ve yapısal yorum [Some new data for southern Menderes Massif and their structural interpretation]. *Jeoloji Mühendisliği* **10**, 9–17.

CANDAN, O. 1995. Menderes Masifi'ndeki kalıntı granulit fasiyesi metamorfizması [Relict granulite-facies metamorphism in the Menderes Massif]. *Turkish Journal of Earth Sciences* **4**, 35–55 [in Turkish with English abstract].

CANDAN, O. 1996. Çine asmasifindeki (Menderes Masifi) gabroların metamorfizması ve diğer asmasiflerle karşılaştırılması [Metamorphism of gabbros in the Çine submassif (Menderes Massif) and it comparison with other submassifs]. *Turkish Journal of Earth Sciences* **5**, 123–39 [in Turkish with English abstract].

CANDAN, O. & DORA, O.Ö. 1998. Granulite, eclogite and blueschist relics in the Menderes Massif: An approach to Pan-African and Tertiary metamorphic evolution. *Geological Society of Turkey Bulletin* **41**, 1–36 [in Turkish with English abstract].

CANDAN, O., DORA O.Ö., OBERHÄNSLI, R., ÇETİNKAPLAN, M., PARTZSCH, J.H., WARKUS, F.C. & DÜRR, S. 2001. Pan-African high-pressure metamorphism in the Precambrian basement of the Menderes Massif, western Anatolia, Turkey. *International Journal of Earth Sciences* **89**, 793–811.

CANDAN, O., OBERHÄNSLI, R., DORA, O.Ö., PARTZSCH, J. & ÇETİNKAPLAN, M. 2000. Polyphase tectono-metamorphic evolution of the Pan-African basement of the Menderes massif: granulite, eclogite and amphibolite facies metamorphism. *Abstracts, IESCA-2000, International Earth Sciences Colloquium on the Aegean Region, İzmir*, p. 134.

CHAPPELL, B.W. & WHITE, A.J.R. 1974. Two contrasting granite types. *Pacific Geology* **8**, 173–174.

CHEN, F., HEGNER, E. & TODT, W. 2000. Zircon ages, Nd isotopic and chemical compositions of orthogneisses from the Black Forest, Germany evidence for a Cambrian magmatic arc. *International Journal of Earth Sciences* **88**, 791–802.

COCHERIE, A., GUERROT, C. & ROSSI, P. 1992. Single-zircon dating by step-wise Pb evaporation: Comparison with other geochronological techniques applied to the Hercinian granites of Corsica, France. *Chemical Geology* **101**, 131–141.

COLEMAN, R.G. & PETERMAN, Z.E. 1975. Oceanic plagiogranite. *Journal of Geophysical Research* **80**, 1099–1108.

COX, K.G., BELL, J.D. & PANKHURST, R.J. 1979. *The Interpretation of Igneous Rocks*. George, Allen and Unwin, London.

DALZIEL, I.W.D. 1997. Neoproterozoic-Paleozoic geography and tectonics: Review, hypothesis, environmental speculation. *Geological Society of America Bulletin* **109**, 16–42.

DANNAT, C. 1997. *Geochemie, Geochronologie und Nd-Sr-Isotopie der granitoiden Kerngneise des Menderes Massivs, SW-Türkei.* Dissertation zur Erlangung des Grades, Doktor der Naturwissenschaften, Johannes Gutenberg-Universität, Mainz.

DANNAT, C. & REISCHMANN, T. 1998. Geochronological, geochemical and isotopic data on granitic gneisses from the Menderes Massif, SW Turkey. *3rd International Turkish Geology Symposium, Ankara, Abstracts*, p. 275.

DE LA ROCHE, H., LETERRIER, J., GRANDCLAUDE, P., & MARCHAL, M. 1980. A classification of volcanic and plutonic rocks using R1-R2 diagram and major element analyses; its relationships with current nomenclature. *Chemical Geology* **29**, 183–210.

DORA, O.Ö. 1975. Menderes Masifi'nde alkali feldspatların yapısal durumları ve bunların petrojenetik yorumlarda kullanılması [Structural interpretation of alkali feldspars in the Menderes Massif and their usage in petrogenetic interpretation]. *Geological Society of Turkey Bulletin* **24**, 91–94 [in Turkish with English abstract].

DORA, O.Ö. 1976. Die Feldspäte als petrogenetischer Indikator im Menderes Massiv/West Anatolien. *Neues Jahrbuch Mineralogie Abhandlungen* **127**, 289–310.

DORA, O.Ö., CANDAN, O., KUN, N., KORALAY, E. & AKAL, C. 1994. Ödemiş-Kiraz Asmasifi'ndeki yeni jeolojik bulgular ve sorunlar [New geologic findings and problems in the Ödemiş-Kiraz submassif]. *Abstracts, 47th Geological Congress of Turkey*, 32–33.

DORA, O.Ö., CANDAN, O., OBERHÄNSLI, R. & DÜRR, ST. 1995. New evidence on the geotectonic evolution of the Menderes Massif. *In*: PIŞKIN, O., ERGÜN, M., SAVAŞÇIN, M.Y. & TARCAN, G. (eds), *Proceedings of International Earth Sciences Colloquium on the Aegean Region*, İzmir **1**, 53–72.

DORA, O.Ö., KUN. N. & CANDAN, O. 1990. Metamorphic history and geotectonic evolution of the Menderes Massif. *In*: SAVAŞÇIN, M.Y. & ERONAT, H. (eds), *Proceedings of International Earth Sciences Colloquium on the Aegean Region*, İzmir **2**, 102–115.

DÜRR, S. 1975. *Über Alter und geotektonische Stellung des Menderes Kristallins/SW-Anatolien und seine Equivalente in der Mittleren Aegeis*. Habilitation thesis. University of Marburg.

DÜRR, S., ALTHER, R., KELLER, J., OKRUSCH, M. & SEIDEL, E. 1978. The median Aegean crystalline belt: Stratigraphy, structure, metamorphism, magmatism. *In*: CLOSS, H., ROEDER, D.R. & SCHMIDT, E. (eds), *Alps, Apennines, Hellenides, Schweizerbart, Stuttgart,* 445–477.

EL BOUSEILY, A.M. & EL SOKKARY, A.A. 1995. The relation between Rb, Ba and Sr in granitic rocks. *Chemical Geology* **16**, 207–219.

ERDOĞAN, B. 1992. Problem of core-mantle boundary of Menderes Massif. *In*: ANIL, M. & NAZİK, A. (eds), *Proceedings of the International Symposium on Eastern Mediterranean Geology,* Adana, Geosound, 314–315.

ERDOĞAN, B. 1993. Menderes Masifi'nin kuzey kanadının stratigrafisi ve çekirdek örtü ilişkisi [Stratigraphy of the northern margin of the Menderes Massif and the core-mantle relations]. *Geological Congress of Turkey, Abstracts*, p. 56.

GARRELS, R.M. & MCKENZIE, F.T. 1971. *Evolution of Sedimentary Rocks*. W. W. Norton New York, NY.

GESSNER, K., COLLINS, A.S., RING, U. & GÜNGÖR, T. 2004. Structural and thermal history of poly-orogenic basement: U–Pb geochronology of granitoid rocks in the southern Menderes Massif, western Turkey. *Journal of the Geological Society, London* **161**, 93–101.

GESSNER, K., PIAZOLO, S., GÜNGÖR, T., RING, U., KRÖNER, A. & PASSCHIER, C.W. 2001b. Tectonic significance of deformation patterns in granitoid rocks of the Menderes nappes, Anatolide belt, southwest Turkey. *International Journal of Earth Sciences* **89**, 766–780.

GESSNER, K., RING, U., JOHNSON, C., HETZEL, R., PASSCHIER, C.W. & GÜNGÖR, T. 2001c. An active bivergent rolling-hinge detachment system: Central Menderes Metamorphic Core Complex in western Turkey. *Geology* **29**, 611–614.

GESSNER, K., RING, U., PASSCHIER, C.W. & GÜNGÖR, T. 2001a. How to resist subduction: evidence for large-scale out-of-sequence thrusting during Eocene collision in western Turkey. *Journal of the Geological Society, London* **158**, 769–784.

GRACIANSKY, P. 1965. Menderes Masifi'nin güney kıyısı boyunca (Türkiye'nin GB'sı) görülen metamorfizma hakkında açıklamalar [Explanation about the metamorphic evolution of the Menderes Massif along the southern border]. *General Directorate of Mineral Research and Exploration Institute of Turkey (MTA) Bulletin* **64**, 8–22 [in Turkish with English abstract].

GÜNGÖR, T. & ERDOĞAN, B. 2002. Tectonic significance of mafic volcanic rocks in a Mesozoic sequence of the Menderes Massif, West Turkey. *International Journal of Earth Sciences* **91**, 386–97.

HEFFERAN, K.P., ADMOU, H., KARSON, J.S. & SAQUAQUE, A. 2000. Anti-Atlas (Morocco) role in Neoproterozoic western Gondwana reconstruction. *Precambrian Research* **103**, 89–96.

HETZEL, R. & REISCHMANN, T. 1996. Intrusion age of Pan-African augen gneiss in the southern Menderes Massif and the age of cooling after Alpine ductile extensional deformation. *Geological Magazine* **133**, 565–572.

HETZEL, R., RING, U., AKAL, C. & TROESCH, M. 1995a. Miocene NNE-directed extensional unroofing in the Menderes Massif, southwestern Turkey. *Journal of the Geological Society, London* **152**, 639–654.

HETZEL, R., PASSCHIER, C.W., RING, U. & DORA, O.Ö. 1995b. Bivergent extension in orogenic belts: the Menderes Massif (southwestern Turkey). *Geology* **23**, 455–458.

HETZEL, R., ROMER, R.L., CANDAN, O. & PASSCHIER, C.W. 1998. Geology of the Bozdağ area, central Menderes Massif, SW Turkey: Pan-African basement and Alpine deformation. *International Journal of Earth Sciences* **87**, 394–406.

HOFMANN, P.F. 1991. Did the breakout of Laurentia turn Gondwana inside out? *Science* **252**, 1409–1412.

IRVINE, T.N. & BARAGAR, W.R.A. 1971. A guide of to the geochemical classification of the common volcanic rocks. *Canadian Journal of Earth Sciences* **8**, 523–548.

IŞIK, V. & TEKELİ, O. 2001. Late orogenic crustal extension in the northern Menderes Massif (western Turkey): evidence for metamorphic core complex formation. *International Journal of Earth Sciences* **89**, 757–65.

IŞIK, V., SEYİTOĞLU, G. & ÇEMEN, İ. 2003. Ductile-brittle transition along the Alaşehir detachment fault and its structural relationship with the Simav detachment fault, Menderes Massif, western Turkey. *Tectonophysics* **374**, 1–18.

JACOBSHAGEN, V. 1986. *Geologie von Griechenland. Berlin:* Gebrüder Borntraeger.

JUNG, S., HOERNES, S. & MEZGER, K. 2000. Geochronology and petrogenesis of Pan-African, syn-tectonic, S-type and post-tectonic A-type granite (Namibia): products of melting of crustal sources, fractional crystallization and wall rock entrainment. *Lithos* **50**, 259–287.

KOBER, B. 1986. Whole-grain evaporation for $^{207}Pb/^{206}Pb$-age-investigations on single zircons using a double-filament thermal ion source. *Contributions to Mineralogy and Petrology* **93**, 482–490.

KOBER, B. 1987. Single-zircon evaporation combined with Pb+ emitter bedding for $^{207}Pb/^{206}Pb$-age investigations using thermal ion mass spectrometry and implications for zirconology. *Contributions to Mineralogy and Petrology* **96**, 63–71.

KOÇYİĞİT, A., YUSUFOĞLU, H. & BOZKURT, E. 1999. Evidence from the Gediz graben for episodic two-stage extension in western Turkey. *Journal of the Geological Society, London* **156**, 605–616.

KONAK, N. 1985. A discussion on the core-cover relationships on the basis of recent observations (Menderes Massif). *Geological Congress of Turkey, Abstracts*, p. 33.

KONAK, N., AKDENİZ, N. & ÖZTÜRK, E.M. 1987. Geology of the south of Menderes Massif. In: *IGCP Project No: 5, Correlation of Variscan and pre-Variscan Events of the Alpine Mediterranean Mountain Belt.* Field meeting, Turkey, 42–53.

KONAK, N., ÇAKMAKOĞLU. A., ELİBOL, E., HAVZAOĞLU, T., HEPŞEN, N., KARAMANDERESİ, I.H., KESKİN, H., SARIKAYA, H., SAV, H. & YUSUFOĞLU, H. 1994. Development of thrusting in the median part of the Menderes Massif. *47th Geological Congress of Turkey, Abstracts,* p. 34.

KORALAY, O.E. 2001. *Geology, Geochemistry and Geochronology of Granitic Gneisses and Leucocratic Orthogneisses at Eastern Part of Ödemiş-Kriaz Submassif, Menderes Massif: Pan-African and Triassic Magmatic Activities*. PhD Thesis, Dokuz Eylül University, İzmir, Turkey [unpublished].

KORALAY, O.E. & DORA, O.Ö. 1999. Menderes Masifi'nde Derbent (Alaşehir) yöresinin jeolojisi ve olasılı Kimmeriyen metamorfizması [Geology and possible Cimmerian metamorphism of Derbent (Alaşehir) region in the Menderes Massif] *Geosound (Yerbilimleri)* **34**, 151–172 [in Turkish with English abstract].

KORALAY, O.E., DORA, O.Ö., CANDAN, O., CHEN, F. & SATIR, M. 2003. Menderes Masifindeki paragnaysların ilksel çökelme yaşına tek zircon $^{207}Pb/^{206}Pb$ evaporasyon jeokronolojisi yöntemiyle yaklaşım. *56th Geological Congress of Turkey, Abstracts*, 64–65.

KORALAY, O.E., SATIR, M. & DORA, O.Ö. 1998. Geochronologic evidence of Triassic and Precambrian magmatism in the Menderes Massif, west Turkey. *3rd International Turkish Geology Symposium, Abstracts*, p. 285.

KORALAY, O.E., SATIR, M. & DORA, O.Ö. 2001. Geochemical and geochronological evidence for Early Triassic calc-alkaline magmatism in the Menderes Massif, western Turkey. *International Journal of Earth Sciences* **89**, 822–835.

KROGH, T.E. 1982. Improved accuracy of U-Pb zircon dating by selection of more concordant fractions using a high gradient magnetic separation technique. *Geochimica et Cosmochimica Acta* **46**, 631–635.

KRÖNER, A., BRAUN, I. & JAEKEL, P. 1996. Zircon geochronology of anatectic melts and residues from a high-grade pelitic assemblage at Ihosy, southern Madagascar: evidence for Pan-African granulite metamorphism. *Geological Magazine* **133**, 311–323.

KRÖNER, A., LINNEBACHER, P., STERN, R.J., REISCHMANN, T., MANTON, W. & HUSSEIN, I.M. 1991. Evolution of the Pan-African island arc assemblages in the southern Red Sea Hills, Sudan and in southwestern Arabia as exemplified by geochemistry and geochronology. *Precambrian Research* **53**, 99–118.

KRÖNER, A. & ŞENGÖR, A.M.C. 1990. Archean and Proterozoic ancestry in late Precambrian to early Paleozoic crustal elements of southern Turkey as revealed by single-zircon dating. *Geology* **18**, 1186–1190.

KRÖNER, A., STERN, R.J. & FLECK, R.J. 1983. Chronology and mechanism of Pan-African crustal accretion in northeast Africa and Arabia, *12th Colloquium on African Geology, Tervuren, Belgium*, 65–78.

KRÖNER, A. & TODT, W. 1988. Single zircon dating constraining the maximum age of the Barberton Greenstone Belt, *South African Journal of Geophysical Research* **93**, 15329–15337.

KUN, N. 1983. *Çine Dolayının Petrografisi ve Menderes Masifi'nin Güney Kesimine Ait Petrolojik Bulgular [Petrography Around Çine Region and Petrologic Findings of Southern Menderes Massif]*. PhD Thesis, Dokuz Eylül University, İzmir, [unpublished].

KUN, N. & CANDAN, O. 1987. *Ödemiş-Kiraz Asmasifi'ndeki Leptitlerin Dağılımı, Konumları ve Oluşum Koşulları [Distribution, Lithostratigraphy and Metamorphism of the Leptites in the Ödemiş-Kiraz Submassif]*. TÜBİTAK Project, Project No: **TBAG 688**.

KUNO, H. 1968. Differantiation of basalt magmas. *In*: HESS, H.H. & POLDERVAART, A. (eds), Basalts: *The Poldervaart Treatise on Rocks of Basaltic Composition*. Wiley Interscience, New York, **2**, 623–688.

LIPS, A.L.W., CASSARD, D., SÖZBİLİR, H., YILMAZ, H., & WIJBRANS, J.R. 2001. Multistage exhumation of the Menderes Massif, western Anatolia (Turkey). *International Journal of Earth Sciences* **89**, 781–792.

LOOS, S. & REISCHMANN, T. 1999. The evolution of the southern Menderes Massif in SW Turkey as revealed by zircon dating. *Journal of the Geological Society, London* **156**, 1021–1030

MANIAR, P.D. & PICCOLI, P.M. 1989. Tectonic discrimination of granitoids. *Geological Society of America Bulletin* **101**, 635–643.

MARC, D. 1992. Granites and rhyolites from the northwestern USA: temporal variation in magmatic processes and relations to tectonic setting. *Transactions of the Royal Society of Edinburgh, Earth Sciences* **83**, 51–64.

MITTWEDE, S.K., KARAMANDERESİ, İ.H. & HELVACI, C. 1995a. *Tourmaline-Rich Rocks of the Southern Part of the Menderes Massif, Southwestern Turkey*. International Earth Sciences Colloquium on the Aegean Region 1995 Excursion Guide. Dokuz Eylül University, Department of Geological Engineering, İzmir, 25 p.

MITTWEDE, S.K., SINCLAIR, W.D., HELVACI, C. & KARAMANDERESİ, İ.H. 1997. Quartz-tourmaline nodules in leucocratic metagranite, southern flank of the Menderes Massif, SW Turkey. *Tourmaline '97, International Symposium on Tourmaline Abstract Volume*, Czech Republic, 57–58.

MITTWEDE, S.K., SINCLAIR, W.D., KARAMANDERESİ, İ.H. & HELVACI, C. 1995b. Geochemistry of quartz-tourmaline nodules from Irmadan (Muğla-Yatağan), Türkiye. *Abstracts of the Second International Turkish Geology Worshop, September 6–8, 1995, Sivas, Turkey*, p. 74.

MOGHAZI, A.M. 2002. Petrology and geochemistry of Pan-African granitoids, Kab Amiri area, Egypt – implications for tectonomagmatic stages in the Nubian Shield evolution. *Mineralogy and Petrology* **75**, 41–67.

OBERHÄNSLI, R., CANDAN, O., DORA, O.Ö. & DÜRR, S. 1997. Eclogites within the Menderes Massif/western Turkey. *Lithos* **41**, 135–150.

OBERHÄNSLI. R, MONIE, P., CANDAN, O., WARKUS, F., PARTZSCH, J.H. & DORA, O.Ö. 1998. The age of blueschist metamorphism in the Mesozoic cover series of the Menderes Massif. *Schweizerische Mineralogische und Petrographische Mitteilungen* **78**, 309–316.

OKAY, A.İ. 1986. High-presure/low temperature metamorphic rocks of Turkey. *Geological Society America Memoir* **164**, 333–347.

OKAY, A.İ. 2001. Stratigraphic and metamorphic inversions in the central Menderes Massif: a new structural model. *International Journal of Earth Sciences* **89**, 709–27.

OKAY, A.İ. 2002. Reply: Stratigraphic and metamorphic inversions in the central Menderes Massif. A new structural model. *International Journal of Earth Sciences* **91**, 173–178.

OKAY, A.İ., SATIR, M., MALUSKI, H., SİYAKO, M., MONIE, P., METZGER, R., & AKYÜZ, S. 1996. Paleo- and Neo-Tethyan events in northwestern Turkey: Geologic and geochronological constraints. *In*: YIN, A. & HARRISON, M. (eds), *The Tectonic Evolution of Asia*. Cambridge University Press, 420–441.

ÖZER, S. & SÖZBİLİR, H. 2003. Presence and tectonic significance of Cretaceous rudist species in the so-called Permo-Carboniferous Göktepe Formation, central Menderes Massif, western Turkey. *International Journal of Earth Sciences* **92**, 397–404.

ÖZER, S., SÖZBİLİR, H., TANSEL, İ.Ö., TOKER, V. & SARI, B. 2001. Stratigraphy of Upper Cretaceous-Paleocene sequences in the southern Menderes Massif (W. Turkey). *International Journal of Earth Sciences* **89**, 852–866.

ÖZTÜRK, A. & KOÇYİĞİT, A. 1983. Menderes grubu kayalarının temel-örtü ilişkisine yapısal bir yaklaşım (Selimiye-Muğla) [A structural approach to the basement-cover relationship in the Menderes Group rocks (Selimiye-Muğla)] *Geological Society of Turkey Bulletin* **26**, 99–106 [in Turkish with English abstract].

PARTZSCH, J., OBERHÄNSLI, R., CANDAN, O. & WARKUS, F. 1998. The Menderes Massif, W Turkey: a complex nappe pile recording 1.0 Ga of geological history. *3rd International Turkish Geology Symposium, Ankara, Abstracts*, p. 281.

PEARCE, J.A. 1976. Statistical analysis of major element patterns in basalts. *Journal of Petrology* **17**, 15–43.

PEARCE, J.A., HARRIS, N.B.W. & TINDLE, A.G. 1984. Trace element discrimination diagrams for the tectonic interpretation of granitic rocks. *Journal of Petrology* **25**, 956–983.

PIPER, J.D.A. 2000. The Neoproterozoic Supercontinent: Rodinia or Paleopangea. *Earth and Planetary Science Letters* **176**, 131–146.

POLLER, U. 1999. A combination of single zircon dating by TIMS and cathodoluminescence investigations on the same grain: The CLC method – U-Pb geochronology for metamorphic rocks. *In*: PAGEL, M., BARBIN, V., BLANC, P. & OHNENSTETTER (eds), *Cathodoluminescence in Geosciences*. Springer, 401–414.

PUPIN, J.P. 1980. Zircon and granite petrology. *Contributions to Mineralogy and Petrology* **73**, 207–220.

PUPIN, J.P. & TURCO, G. 1972. Une typologie originale du zircon accessoire. *Bulletin de la Societe Francaise de Minéralogie et de Cristallographie* **95**, 348–359.

PUPIN, J.P. & TURCO, G. 1974. Application à quelques roches endogènes du massif franco-italien de l'Argentera-Mercantour, d'une typologie originale du zircon accessoire. Étude comparative avec la méthode des R.M.A. *Bulletin de la Societe Francaise de Minéralogie et de Cristallographie* **97**, 59–69.

RÉGNIER, J.L., RING, U., PASSCHIER, C.W., GESSNER, K. & GÜNGÖR, T. 2003. Contrasting metamorphic evolution of metasedimentary rocks from the Çine and Selimiye nappes in the Anatolide belt, western Turkey. *Journal of Metamorphic Geology* **21**, 699–721.

RIMMELÉ, G., JOLIVET, L., OBERHÄNSLI, R. & GOFFÉ, B. 2003a. Deformation history of the high-pressure Lycian Nappes and implications for tectonic evolution of SW Turkey. *Tectonoics* **22**, 1007–1029.

RIMMELÉ, G., OBERHÄNSLI, R., GOFFÉ, B., JOLIVET, L., CANDAN, O. & ÇETİNKAPLAN, M. 2003b. First evidence of high-pressure metamorphism in the 'Cover Series' of the southern Menderes Massif. Tectonic and metamorphic implications for the evolution of the SW Turkey. *Lithos* **71**, 19–46.

RING, U., GESSNER, K., GÜNGÖR, T. & PASSCHIER, C.W. 1999. The Menderes Massif of western Turkey and the Cycladic Massif in the Aegean - do they really correlate? *Journal of the Geological Society, London* **156**, 3–6.

RING, U., JOHNSON, C., HETZEL, R. & GESSNER, K. 2003. Tectonic denudation of a Late Cretaceous-Tertiary collisional belt: regionally symmetric cooling patterns and their relation to extensional faults in the Anatolide belt of western Turkey. *Geological Magazine* **140**, 421–441.

RING, U. & LAYER, P.W. 2003. High-pressure metamorphism in the Aegean, eastern Mediterranean: Underplating and exhumation from the Late Cretaceous until the Miocene to Recent above the retreating Hellenic subduction zone. *Tectonics* **22**, 1022 (doi: 10.29/2001TC001350).

RING, U., WILLNER, A. & LACKMANN, W. 2001. Stacking of nappes with different pressure-temperature paths: an example from the Menderes nappes of western Turkey. *American Journal of Science* **301**, 912–44.

SALEM, I.A., ABDEL-MONEUM, A.A., SHAZLY, A.G. & EL-SHIBINY, N.H. 2001. Mineralogy and geochemistry of Gabal El-Ineigi Granite and associated fluorite veins, Central Eastern Desert, Egypt: application of fluid inclusions to fluorite genesis. *Journal of African Earth Sciences* **32**, 29–45.

SATIR, M. & FRIEDRICHSEN, H. 1986. The origin and evolution of the Menderes Massif, W-Turkey: A rubidium/strontium and oxygen isotope study. *Geologische Rundschau* **75**, 703–714.

SCHUILING, R.D. 1962. Petrology, age and structure of Menderes Migmatite Complex in southwest Turkey. *General Directorate of the Mineral Research and Exploration Institute of Turkey (MTA) Bulletin* **58**, 71–84.

ŞENGÖR, A.M.C. & YILMAZ, Y. 1981. Tethyan evolution of Turkey: a plate tectonic approach. *Tectonophysics* **75**, 181–241.

ŞENGÖR, A.M.C., SATIR, M. & AKKÖK, R. 1984. Timing of tectonic events in the Menderes Massif, western Turkey: Implications for tectonic evolution and evidence for Pan-African basement in Turkey. *Tectonics* **3**, 693–707.

SEYİTOĞLU, G., ÇEMEN, İ. & TEKELİ, O. 2000. Extensional folding in the Alaşehir (Gediz Graben, western Turkey). *Journal of the Geological Society, London* **157**, 1097–1100.

SEYİTOĞLU, G., SCOTT, B. & RUNDLE, C.C. 1992. Timing of Cenozoic extensional tectonics in west Turkey. *Journal of the Geological Society, London* **149**, 533–538.

SEYİTOĞLU, G., TEKELİ, O., ÇEMEN, İ., ŞEN, Ş. & IŞIK, V. 2002. The role of the flexural rotation/rolling hinge model in the tectonic evolution of the Alaşehir graben, western Turkey. *Geological Magazine* **139**, 15–26.

SHAND, S.J. 1943. *Eruptive Rocks: Their Genesis Composition, Classification, and their Relations to Ore Deposits.* John Wiley, New York.

STACEY, J.S. & KRAMERS, J.D. 1975. Approximation of terrestrial lead isotope evolution by a two stage model. *Earth and Planetary Science Letters* **26**, 207–221.

STEIN, M., & GOLDSTEIN, S.L. 1996. From plume head to continental lithosphere in the Arabian-Nubian shield. *Nature* **382**, 773–778.

STERN, R.J. 1994. Arc assembly and continental collision in the Neoproterozoic East African orogen and implications for the consolidation of Gondwana. *Annual Review of Earth and Planetary Sciences* **22**, 319–351.

SÖZBİLİR, H. 2001. Geometry of macroscopic structures with their relations to the extensional tectonics: field evidence from the Gediz detachment, western Turkey. *Turkish Journal of Earth Sciences* **10**, 51–67.

SÖZBİLİR, H. 2002. Geometry and origin of folding in the Neogene sediments of the Gediz Graben, western Anatolia, Turkey. *Geodinamica Acta* **15**, 277–288.

TACK, L. & BOWDEN, P. 1999. Post-collisional granite magmatism in the central Damaran (Pan-African) Orogenic Belt, western Namibia. *Journal of African Earth Sciences* **28**, 653–674.

TADESE, T., HOSHINO, M., SUZUKI, K. & IIZUMI, S. 2000. Sm-Nd, Rb-Sr and Th-U-Pb zircon ages of syn- and post-tectonic granitoid rocks from the Axum area of northern Ethiopia. *Journal of African Earth Sciences* **30**, 313–327.

TEKLAY, M., KRÖNER, A., MEZGER, K. & OBERHÄNSLI, R. 1998. Geochemistry, Pb-Pb single zircon ages and Nd-Sr isotope composition of Precambrian rocks from southern and eastern Ethiopia: implications for crustal evolution in East Africa. *Journal of African Earth Sciences* **26**, 207–227.

TEKLAY, M., KRÖNER, A. & MEZGER, K. 2001. Geochemistry, geochronology and isotope geology of Nakfa inrusive rocks, northern Eritrea: products of a tectonically thickened Neoproterozoic arc crust. *Journal of African Earth Sciences* **33**, 283–301.

TROMPETTE, R. 1994. *Geology of western Gondwana,* Rotterdam, A.A. Balkema.

UNITED NATIONS, 1974. *Mineral Exploration in Two Areas*. Technical Report **4**, DP/DN, Tur-27-004/4, Turkey.

UNRUG, R. 1996. The assembly of Gondwana. *Episodes* **19**, 11–20.

WHITNEY, D.L. & BOZKURT, E. 2002. Metamorphic history of the southern Menderes Massif, western Turkey. *Geological Society of America Bulletin* **114**, 829–38.

WILSON, M. 1989. *Igneous Petrogenesis*. Unwin Hyman, London.

WINCHESTER, J.A. & FLOYD, P.A. 1977. Geochemical discrimination of different magma series and their differentiation products using immobile elements. *Chemical Geology* **20**, 325–343.

Received 07 August 2002; revised typescript accepted 09 February 2004